

University of Groningen

Bispecific antibody CD73xEGFR more selectively inhibits the CD73/adenosine immune checkpoint on cancer cells and concurrently counteracts pro-oncogenic activities of CD73 and EGFR

Ploeg, Emily Maria; Samplonius, Douwe Freerk; Xiong, Xiao; Ke, Xiurong; Hendriks, Mark Alexander Johannes Martinus; Britsch, Isabel; Van Wijngaarden, Anne Paulien; Zhang, Hao; Helfrich, Wijnand

Published in:
Journal for immunotherapy of cancer

DOI:
[10.1136/jitc-2023-006837](https://doi.org/10.1136/jitc-2023-006837)

IMPORTANT NOTE: You are advised to consult the publisher's version (publisher's PDF) if you wish to cite from it. Please check the document version below.

Document Version
Publisher's PDF, also known as Version of record

Publication date:
2023

[Link to publication in University of Groningen/UMCG research database](#)

Citation for published version (APA):

Ploeg, E. M., Samplonius, D. F., Xiong, X., Ke, X., Hendriks, M. A. J. M., Britsch, I., Van Wijngaarden, A. P., Zhang, H., & Helfrich, W. (2023). Bispecific antibody CD73xEGFR more selectively inhibits the CD73/adenosine immune checkpoint on cancer cells and concurrently counteracts pro-oncogenic activities of CD73 and EGFR. *Journal for immunotherapy of cancer*, 11(9), Article e006837. <https://doi.org/10.1136/jitc-2023-006837>

Copyright

Other than for strictly personal use, it is not permitted to download or to forward/distribute the text or part of it without the consent of the author(s) and/or copyright holder(s), unless the work is under an open content license (like Creative Commons).

The publication may also be distributed here under the terms of Article 25fa of the Dutch Copyright Act, indicated by the "Taverne" license. More information can be found on the University of Groningen website: <https://www.rug.nl/library/open-access/self-archiving-pure/taverne-amendment>.

Take-down policy

If you believe that this document breaches copyright please contact us providing details, and we will remove access to the work immediately and investigate your claim.

Bispecific antibody CD73xEGFR more selectively inhibits the CD73/adenosine immune checkpoint on cancer cells and concurrently counteracts pro-oncogenic activities of CD73 and EGFR

Emily Maria Ploeg ¹, Douwe Freerk Samplonius ¹, Xiao Xiong^{2,3}, Xiurong Ke ^{1,4}, Mark Alexander Johannes Martinus Hendriks ¹, Isabel Britsch ¹, Anne Paulien van Wijngaarden ¹, Hao Zhang ^{5,6}, Wijnand Helfrich ¹

To cite: Ploeg EM, Samplonius DF, Xiong X, *et al*. Bispecific antibody CD73xEGFR more selectively inhibits the CD73/adenosine immune checkpoint on cancer cells and concurrently counteracts pro-oncogenic activities of CD73 and EGFR. *Journal for ImmunoTherapy of Cancer* 2023;11:e006837. doi:10.1136/jitc-2023-006837

► Additional supplemental material is published online only. To view, please visit the journal online (<http://dx.doi.org/10.1136/jitc-2023-006837>).

Accepted 15 August 2023



© Author(s) (or their employer(s)) 2023. Re-use permitted under CC BY-NC. No commercial re-use. See rights and permissions. Published by BMJ.

For numbered affiliations see end of article.

Correspondence to Prof. Dr. Wijnand Helfrich; w.helfrich@umcg.nl

Dr. Emily Maria Ploeg; e.m.ploeg@umcg.nl

ABSTRACT

Background CD73 is an ecto-enzyme that is involved in the conversion of pro-inflammatory extracellular ATP (eATP) excreted by cancer cells under stress to anti-inflammatory adenosine (ADO). A broad variety of solid cancer types was shown to exploit CD73 overexpression as a suppressive immune checkpoint. Consequently, CD73-antagonistic antibodies, most notably oleclumab, are currently evaluated in several multicenter trials for clinical applicability. However, the efficacy of conventional monospecific CD73-inhibiting antibodies may be limited due to on-target/off-tumor binding to CD73 on normal cells. Therefore, a novel approach that more selectively directs CD73 immune checkpoint inhibition towards cancer cells is warranted.

Methods To address this issue, we constructed a novel tetravalent bispecific antibody (bsAb), designated bsAb CD73xEGFR. Subsequently, the anticancer activities of bsAb CD73xEGFR were evaluated using in vitro and in vivo tumor models.

Results In vitro treatment of various carcinoma cell types with bsAb CD73xEGFR potently inhibited the enzyme activity of CD73 (~71%) in an EGFR-directed manner. In this process, bsAb CD73xEGFR induced rapid internalization of antigen/antibody complexes, which resulted in a prolonged concurrent displacement of both CD73 and EGFR from the cancer cell surface. In addition, bsAb CD73xEGFR sensitized cancer to the cytotoxic activity of various chemotherapeutic agents and potently inhibited the proliferative/migratory capacity (~40%) of cancer cells. Unexpectedly, we uncovered that treatment of carcinoma cells with oleclumab appeared to enhance several pro-oncogenic features, including upregulation and phosphorylation of EGFR, tumor cell proliferation (~20%), and resistance towards cytotoxic agents and ionizing radiation (~39%). Importantly, in a tumor model using immunocompetent BALB/c mice inoculated with syngeneic CD73^{pos}/EGFR^{pos} CT26 cancer cells, treatment with bsAb CD73xEGFR outperformed oleclumab (65% vs 31% tumor volume reduction). Compared with oleclumab, treatment with bsAb CD73xEGFR enhanced the intratumoral presence of CD8^{pos} T cells and M1 macrophages.

Conclusions BsAb CD73xEGFR outperforms oleclumab as it inhibits the CD73/ADO immune checkpoint in an EGFR-directed manner and concurrently counteracts several oncogenic activities of EGFR and CD73. Therefore, bsAb CD73xEGFR may be of significant clinical potential for various forms of difficult-to-treat solid cancer types.

BACKGROUND

Immunotherapy has significantly contributed to the therapeutic armamentarium currently available to patients with cancer with advanced disease. In particular, antagonistic antibodies towards immune checkpoints programmed cell death protein 1 (PD-1)/programmed cell death ligand 1 (PD-L1) and cytotoxic T-lymphocyte-associated antigen 4 (CTLA-4) have strongly improved therapeutic outcome, although only for a relatively small subgroup of these patients. Apparently, the majority of patients with cancer harbor malignant cells that exploit alternate and/or additional immunosuppressive checkpoints to achieve immune evasion. Consequently, there is an unmet need for novel inhibitors that can selectively block such alternate immune checkpoints. In this respect, antagonistic antibodies that can selectively inhibit the CD73 immune checkpoint, such as oleclumab, appear to be of clinical promise.^{1,2}

CD73 is a cell surface-expressed enzyme that is key in maintaining immune system homeostasis by the stepwise hydrolysis of the autocrine and paracrine danger signals conveyed by extracellular ATP (eATP) into anti-inflammatory adenosine (ADO). Infection, tissue injury, ischemia, and metabolic stress are known to result in a sharp elevation of eATP release at the site of such lesion(s),

WHAT IS ALREADY KNOWN ON THIS TOPIC

⇒ Inhibition of the CD73 immune checkpoint has been hailed as a promising alternate or complementary approach in cancer immunotherapy. However, recent midterm clinical trial reports indicate that, as a single treatment modality, the efficacy of CD73 antagonistic antibody oleclumab remains modest at best.

WHAT THIS STUDY ADDS

⇒ A novel tetravalent bispecific antibody (bsAb) CD73xEGFR is presented that allows to inhibit the CD73/adenosine immune checkpoint on cancer cells in an EGFR-directed manner. Its mode-of-action involves the rapid co-internalization and prolonged concurrent displacement of CD73 and EGFR from the cancer cell surface. BsAb CD73xEGFR showed potent capacity to reinvigorate the anticancer activities of adenosine-suppressed cytotoxic T cells and concurrently counteracted cancer cell-surface CD73-mediated and EGFR-mediated pro-oncogenic activities. Of note, we uncovered that identical treatment of carcinoma cells with CD73-antagonistic antibody oleclumab appeared to enhance several pro-oncogenic features, including the upregulation and phosphorylation of EGFR, enhancement of tumor cell proliferation, and promotion of resistance towards chemotherapeutic agents and ionizing radiation.

HOW THIS STUDY MIGHT AFFECT RESEARCH, PRACTICE OR POLICY

⇒ The uncovered negative attributes of CD73 antagonistic antibody oleclumab can have major ramifications for its future application in cancer treatment. Therefore, alternate approaches that inhibit the CD73 immune checkpoint in a more tumor-selective manner while counteracting the pro-oncogenic activity of EGFR and CD73 appear warranted. In this respect, the multiple and more tumor-selective anticancer activities of bsAb CD73xEGFR may be of particular promise.

where it serves to initiate pro-inflammatory immune responses by attracting and activating various types of immune cells. These pro-inflammatory responses are appropriately locally counterbalanced by the concerted action of cell surface-anchored ectonucleotides CD39 and CD73, which sequentially convert eATP via AMP to ADO. In this process, the enzyme activity of CD73 is the rate-limiting step in catalyzing the conversion of AMP to ADO. This catalysis results in a rapid local increase of ADO levels, which engages the immunosuppressive actions of ADO receptors on various, locally present immune cells, thereby providing a self-limiting mechanism for a timely and localized resolution of immune responses.¹

Due to intrinsic high metabolic stress, numerous cancer cell types excrete remarkably high levels of pro-inflammatory eATP, which they rapidly convert into anti-inflammatory ADO by concurrently overexpressing CD73. Subsequently, diffusion of tumor-produced ADO molecules results in the formation of a potent immunosuppressive “halo” that acts not only locally in the tumor microenvironment, but also outside of the tumor site. Consequently, a halo of ADO molecules chronically suppresses the anticancer immune response, which promotes the induction of immune tolerance, immune escape, and subsequent cancer progression.³

Preclinical studies have demonstrated that CD73-inhibiting antibodies may be used to overcome this form of tumor-induced immunosuppression in a broad variety of cancer types, including various carcinomas. In particular, oleclumab (MEDI9447), a recombinant fully human antibody, selectively binds to CD73 and subsequently inhibits its enzyme activity.⁴ Currently, several multicenter trials are ongoing in patients with advanced solid malignancies to evaluate the clinical potential of oleclumab. However, the efficacy of a conventional monospecific CD73-inhibiting antibody like oleclumab is anticipated to be hampered by the “on-target/off-tumor” binding to a vast surplus of CD73 molecules present on normal cells and tissues,⁵ potentially precluding its sufficient accumulation at the tumor site(s). Moreover, CD73-inhibiting antibodies may induce a generalized (re-)activation of T cells, potentially leading to autoimmune-related adverse events, analogous to what is observed for other immune checkpoint inhibitors.

Intriguingly, we uncovered that *in vitro* treatment of carcinoma cells with oleclumab induced upregulation and phosphorylation of oncogenic proteins EGFR and HER2, which coincided with a marked enhancement of cancer cell proliferation and resistance towards cytotoxic regimes.

To address these issues, we constructed a novel tetravalent bispecific antibody (bsAb), designated “bsAb CD73xEGFR”, that was engineered to inhibit cancer cell surface-expressed CD73 in an EGFR-directed manner. Our results demonstrate that treatment with bsAb CD73xEGFR reduced the outgrowth of inoculated syngeneic tumors in immunocompetent mice, which coincided with a marked increase in tumor-infiltration by CD8^{pos} effector T cells and activated macrophages. Moreover, bsAb CD73xEGFR sensitized cancer to the cytotoxic activity of various chemotherapeutic agents and that of ionizing radiation *in vitro* and potently inhibited the proliferative and migratory capacity of cancer cells *in vivo*.

METHODS

Antibodies and reagents

Antibodies: Fluorescein isothiocyanate (FITC)-labeled anti-CD73 (clone-MM07, Sino Biological), Allophycocyanin (APC)-labeled anti-EGFR (clone-528, Santa Cruz), FITC-labeled-annexin-V (ImmunoTools), goat anti-human-IgG-APC (SouthernBiotech), sheep anti-human-CD73 (R&D), rabbit anti-human-EGFR (Abcam), rabbit anti-human-HER2 (R&D), rabbit anti-human/mouse- β -Actin (Abcam), rabbit anti-sheep-IgG (Thermo Fisher), goat anti-rabbit-IgG (Dako), anti-CD4 (ab183685, Abcam), anti-CD8 (98941, Cell Signaling Technology), anti-FoxP3 (ab99964; Abcam), anti-F4/80 (ab240946, Abcam), anti-CD206 (ab64693, Abcam), anti-CD11c (ab52632; Abcam).

Reagents/proteins: VivoGlo (Promega), Carboxy-fluorescein succinimidyl ester (CFSE), CFSE-Far Red (Thermo Fisher), Vybrant DiD, DiO, propidium iodide

(PI), fluorescent caspase 3/8–488 probe (Biotium), adenosine 5'-(α,β -methylene)diphosphate (APCP, Sigma), anti-human Fc saporin-6 toxin-labeled Fab (Fab-ZAP, Advanced Targeting Systems), CypHer5E (Fisher Scientific), AMP (Sigma-Aldrich), T-cell activation/expansion beads (Miltenyi Biotec), recombinant soluble human-CD73 (s.hCD73) (Abcam), interferon (IFN)- γ ELISA (eBioscience), colorimetric malachite green-based inorganic phosphate (Pi) (ab65622, Abcam).

Cell lines and transfectants

Cell lines CHO-K1, SK-BR-3, 4T1, FaDu, H292, OvCAR3, H322, PC3M, A375m, A2058, SK-MEL-28, MDA-MB-231, DLD1, CT26, and HEK293AD were obtained from the American Type Culture Collection (Manassas, Virginia, USA). A549, A549.EGFR-KO,⁶ H1650, and H1650 EGFR-KO were kindly provided by Professor Dr H J Haisma. H292-luc cancer cells were purchased from Cellomics Technology (SC-1087).

Cells were cultured in Roswell Park Memorial Institute (RPMI)-1640 or Dulbecco's Modified Eagle Medium (DMEM) (Lonza), supplemented with 10% fetal calf serum (Thermo Fisher) at 37°C in a humidified 5% CO₂ atmosphere. CHO-K1 cells were cultured in GMEM (FirstLink), supplemented with 5% dialyzed fetal bovine serum (Sigma-Aldrich).

CHO.CD73 cells stably expressing human CD73 were generated by lipofection (FuGENE-HD, Promega) of a plasmid containing complementary DNA (cDNA) encoding human CD73 (OriGene). Likewise, CHO.EGFR cells were generated by lipofection of a plasmid containing cDNA encoding human EGFR (Sino Biological).

CD73-knockout (KO) cells were generated using CRISPR-Cas9 by transfection of pSpCas9 BB-2A-GFP (PX458) plasmid (Addgene plasmid #48138) containing CD73-targeting sgRNA 5'-GCAGCACGTTGGGTTCCGGCG-3'.⁷ Likewise, EGFR-KO cells were generated by transfection of pSpCas9 BB-2A-GFP (PX458) plasmid containing EGFR-targeting sgRNA 5'-GAGTAACAAGCTCAGG-CAGT-3' (GenScript).

Construction of bsAb CD73xEGFR-IgG2 silent

DNA fragments encoding scFvCD73 and VHH-EGFR were generated by commercial gene synthesis service (GenScript) based on published VH and VL sequence data from oleclumab⁴ and EGFR-directed camelid single-domain antibody fragment NRC-sdAb028,⁸ respectively. For construction of bsAb CD73xEGFR-IgG2 silent and controls, we refer to the supplementary documentation.

Production of recombinant bsAbs

BsAbs were produced using the Expi293 Expression System (Thermo Fisher) and purified using ÄKTA-Start chromatography system as described previously by our group.⁹

Assessment dual binding activity of bsAb CD73xEGFR

Cancer cells were incubated at given concentration with bsAbs CD73xEGFR or controls at 4°C for 45 min.

Subsequently, cells were re-incubated with APC-labeled secondary anti-human-Ig-antibody at 4°C for 45 min. Binding data of the respective bsAbs were acquired using Guava easyCyte 6/2L Flow Cytometer (Merck Millipore) and analyzed by GuavaSoft V.3.2 software.

Similar, competitive binding of bsAb CD73xEGFR (1 μ g/mL) was assessed in the presence of either recombinant soluble human CD73 (s.CD73), EGFR-competing bsAb MockxEGFR, or a combination thereof (each 10 μ g) at 4°C for 20 min and evaluated by flow cytometry essentially as described above.

Assessment of internalization of bsAb CD73xEGFR/antigen complexes

Cancer were incubated with increasing concentrations (0.01–10 μ g/mL) bsAb CD73xEGFR (or appropriate controls) at 37°C for 24 hours, after which residual CD73-cell and EGFR-cell-surface exposure was assessed using anti-CD73 mAbMM07 and anti-EGFR mAb528, which bind to non-overlapping epitopes on CD73 and EGFR, respectively.

Cancer cells were incubated with bsAb CD73xEGFR-pHAb (CypHer5E) or controls (1 μ g/mL) in the presence (or absence) of EGFR-competing bsAb MockxEGFR (10 μ g/mL) at 37°C for 0 min, 10 min, 60 min, 240 min, or 360 min. CypHer5E is a non-toxic, pH-sensitive dye that is non-fluorescent at basic pH (extracellular: culture medium) and fluorescent at acidic pH (intracellular: endosomes, lysosomes). Internalization of pHAb-labeled bsAbs by cancer cells was evaluated by flow-cytometry.

Cancer cells were incubated with bsAb CD73xEGFR or controls (1 μ g/mL) in the presence of anti-human Fc saporin-6 toxin-labeled Fab (Fab-ZAP, Advanced Targeting Systems). Fab-ZAP is a goat anti-human IgG (H+L) monovalent Fab antibody fragment conjugated with the pro-apoptotic ribosome-inactivating protein saporin. The pro-apoptotic activity of the “Fab-ZAP” agent strictly depends on its internalization. Apoptotic cancer cell death was evaluated after 24 hours by flow-cytometry using annexin-V/PI staining.

Assessment capacity of bsAb CD73xEGFR to inhibit the enzyme activity of CD73

Pi formed during CD73-mediated hydrolysis of AMP to ADO was measured using a colorimetric malachite green-based Pi assay as described previously by our group.⁹ Additionally, we refer to the online supplemental files 1; 3.

Assessment capacity of bsAb CD73xEGFR to restore proliferation capacity of ADO-suppressed T cells

CFSE-labeled peripheral blood mononuclear cells (PBMCs) were activated by addition of T-cell activation/expansion beads in a bead-to-cell ratio of 1:1. Subsequently, PBMCs were cultured in medium supplemented (or not) with AMP (100 μ M) and incubated with bsAb CD73xEGFR or controls (1 μ g/mL) for 5 days. T-cell proliferation was analyzed by CFSE dilution using flow-cytometry.

Similarly, proliferation of CFSE-Far Red-labeled PBMCs evaluated using live cell imaging was performed as described previously by our group.⁹

Assessment capacity of bsAb CD73xEGFR to restore anticancer activity of ADO-suppressed T cells in vitro

PBMCs were cultured in a medium supplemented with AMP (100 μ M) and incubated with increasing concentrations (0.01–10 μ g/mL) bsAb CD73xEGFR or controls for 24 hours. Next, the T cells present were stimulated and re-directed to kill epithelial cell adhesion molecule (EpCAM)-expressing PC3M prostate cancer cells and evaluated using live cell imaging as described previously by our group.⁹

Assessment capacity of bsAb CD73xEGFR to restore anticancer activity of ADO-suppressed T cells in vivo

Syngeneic tumors were established by subcutaneous injection of 5×10^5 CT26 cells suspended in 0.1 mL of phosphate buffered saline (PBS) into the right flanks of 4–6 weeks old female BALB/c mice (Janvier, France). Animals were randomized using RandoMice into five groups of nine mice each based on body weight (total=45 animals). Sample size was determined using G*Power tool). BsAb CD73xEGFR and controls were administered by intraperitoneal (I.P.) injection at 7.5 mg/kg on days 4, 7, 10, and 14. Tumor volume was assessed by caliper measurements. Mice were euthanized using cardiac puncture, followed by cervical dislocation after 21 days. Tumor and organs and processed for multiplexed immunofluorescence or histology.

Multiplexed immunofluorescence to assess tumor-infiltrating leukocytes

Multiplexed immunofluorescence to evaluate T cell and macrophage populations in tumors resected from immunocompetent mice was performed as described previously.¹⁰ Additional information is provided in the online supplemental file 3.

Assessment inhibitory effect of bsAb CD73xEGFR on proliferation of cancer cells in vitro

Cancer cells were seeded into an E-plate 16 (ACEA Biosciences) and incubated with bsAb CD73xEGFR or controls (1 μ g/mL) at 37°C for 60 hours. Cell proliferation was monitored using the xCELLigence RTCA instrument (ACEA Biosciences).

Cancer cells were seeded into a 96-well culture plate and incubated with bsAb CD73xEGFR or controls (1 μ g/mL) at 37°C. Live cell imaging technology (IncuCyte) was used to follow proliferation of cancer cells by taking pictures at 4 \times magnification every 4 hours for 3 days. Confluence (%) was measured using IncuCyte software 2019B.

Assessment inhibitory effect of bsAb CD73xEGFR on proliferative capacity of cancer cells in vivo

Tumors were established by subcutaneous injection of 1×10^6 H292-Luc cells suspended in 0.1 mL of PBS into

the right flanks of a 4–6 weeks old female athymic nude mouse (CrI:NU(NCr)-Foxn1tm, Charles River, Germany). Animals were randomized using RandoMice into five groups of nine mice each based on body weight (total=45 animals). Sample size was determined using G*Power tool). BsAb CD73xEGFR or controls were administered via I.P. injection at 7.5 mg/kg on days 7, 10 and 17. Bioluminescent imaging (IVIS Spectrum, 75 mg/kg VivoGlo; Promega) and caliper measurements were performed to evaluate tumor growth. Mice were euthanized using cardiac puncture, followed by cervical dislocation after 28 days.

Assessment inhibitory effect of bsAb CD73xEGFR on migratory capacity of cancer cells

Cancer cells were seeded in 24-well plates, equipped with a stopper, in the presence of bsAb CD73xEGFR or controls (1 μ g/mL) at 37°C for 24 hours. Subsequently, the stopper was removed and Live Cell Imaging technology (IncuCyte) was used to assess the treatment effect on the migratory capacity of cancer cells by taking pictures at 4 \times magnification every 0.5 hours for 3 days. Closure of the standardized cell-free zone (%) was measured using IncuCyte software 2019B.

Assessment capacity of bsAb CD73xEGFR to sensitize cancer cells towards chemotherapeutic agents and radiation

Cancer cells were seeded into a 96-well culture plate and incubated with bsAb CD73xEGFR or controls (1 μ g/mL) with (or without) 5FU (50 μ g/mL), taxol (50 nM), cisplatin (1 μ g/mL), or doxorubicin (50 nM) at 37°C. Live Cell Imaging technology (IncuCyte) was used to assess treatment effect on proliferative capacity on cancer cells by taking pictures at 4 \times magnification every 6 hours for 6 days. Confluence (%) was measured using IncuCyte software 2019B.

Cancer cells were seeded into a 6-well culture plate and incubated with increasing concentrations (0.01–10 μ g/mL) of bsAb CD73xEGFR or controls at 37°C for 14 days. Subsequently, cell colonies were washed with PBS and then stained with crystal violet. Colony number and size were analyzed using ImageJ software.

Cancer cells were seeded into a 6-well culture plate, incubated with bsAb CD73xEGFR or controls (1 μ g/mL), irradiated with an increasing dose of radiation (0.5–2 Gy), and then cultured at 37°C for 14 days. Subsequently, cell colonies were washed, stained, and analyzed as described above. Irradiation (0.59 Gy/min) was performed using a ¹³⁷Ce source (IBL637 Cesium-137 γ -ray machine).

Statement animal experiments

All procedures using animals were in accordance with Dutch Act on Animal Experimentation and approved by the Institutional Animal Welfare Committee at the Rijksuniversiteit Groningen/University Medical Center Groningen (AVD1050020209544). EMP was aware of group allocation at the different stages of the experiment (during allocation, conduct of the experiment,

outcome assessment, and data analysis). Additionally, we did not adjust for confounding since randomization was successful.

Statistical analysis

Statistical analysis was done by (multiple) t-test, one-way analysis of variance followed by Tukey post hoc test, or (non-)linear regression, as indicated using Prism software. Data was pooled (n-number and technical repeats are specified in the figure legends) for analysis. P value < 0.05 was defined as a statistically significant difference. Where indicated; ns = p > 0.05; * = p < 0.05; ** = p < 0.01; *** = p < 0.001; **** = p < 0.0001.

RESULTS

bsAb CD73xEGFR has dual binding specificity for CD73 and EGFR

BsAb CD73xEGFR was constructed in the bispecific taFv-Fc format¹¹ equipped with two identical CD73-directed scFv antibody fragments derived from oleclumab and two identical EGFR-directed camelid single-domain antibody fragments⁸ (online supplemental files 1; 3). Dual binding activity of bsAb CD73xEGFR was confirmed using Chinese hamster ovary (CHO) cells transfected with either human CD73 or human EGFR. BsAb CD73xEGFR bound dose-dependently to both CHO.CD73 and CHO.EGFR cells, and not to parental CHO cells (figure 1A). Binding of bsAb CD73xEGFR towards SK-BR-3 breast cancer cells was partly reduced in the presence of soluble human CD73 (s.CD73), whereas antagonistic EGFR bsAb MockxEGFR strongly inhibited the binding. Of note, binding of bsAb CD73xEGFR was fully abrogated in combined presence of s.CD73 and bsAb MockxEGFR (figure 1B), indicating bsAb CD73xEGFR selectively and simultaneously binds to CD73 and EGFR. Importantly, binding levels of bsAb CD73xEGFR towards a panel of four CD73^{pos}/EGFR^{pos} cell lines closely correlated with their respective expression levels for EGFR (figure 1C, online supplemental file 3). Moreover, bsAb CD73xEGFR showed reduced binding activity towards EGFR-KO/CD73^{pos} cell lines (figure 1C). Additionally, bsAb CD73xEGFR showed capacity to simultaneously bind to CD73 present on one cell type and EGFR present on another cell type when both cell types are in close proximity. In particular, bsAb CD73xEGFR cellularly bridged FaDu cancer cells (DiO-labeled) and CHO.CD73 cells (DiD-labeled), as was evident from a marked increase in DiO^{pos}/DiD^{pos} cell clusters detected by flow cytometry (online supplemental file 3).

bsAb CD73xEGFR induces rapid co-internalization and subsequent prolonged displacement of both CD73 and EGFR from the cancer cell surface

Treatment of CD73^{pos}/EGFR^{pos} H292 cancer cells with bsAb CD73xEGFR resulted in a concurrent and dose-dependent cancer cell surface displacement of CD73 and EGFR. At a concentration of 1 µg/mL, treatment with bsAb CD73xEGFR reduced cell surface exposure of CD73 and

EGFR by 81% and 73%, respectively (figure 2A,B, online supplemental file 3), which persisted for up to 96 hours (figure 2C,D). Comparable prolonged displacement of CD73 and EGFR was detected when primary patient-derived ovarian and colon cancer cells were treated with bsAb CD73xEGFR (figure 2E). Internalization of bsAb CD73xEGFR/antigen complexes occurred after 10–60 min, which was abolished in presence of saturating amounts of EGFR-competing bsAb MockxEGFR (figure 2F). Likewise, “piggybacking” of Fab-ZAP toxin on internalizing bsAb CD73xEGFR resulted in saporin-mediated apoptotic cell death (figure 2G). Analogously, treatment of CD73^{pos}/EGFR^{pos} cancer cells with bsAb CD73xEGFR significantly reduced CD73 expression levels and attenuated EGFR tyrosine phosphorylation (online supplemental file 3).

bsAb CD73xEGFR internalizes cancer cell surface-exposed CD73 in an EGFR-directed manner

BsAb CD73xEGFR showed a marked capacity to displace CD73 from CD73^{pos}/EGFR^{pos} cancer cells, whereas only minimal CD73 displacement was observed when treating CD73^{pos}/EGFR^{neg} cancer cells (online supplemental file 3). Analogously, bsAb CD73xEGFR essentially failed to internalize CD73 when treating A549 EGFR-KO and H1650 EGFR-KO cells (online supplemental file 3). Importantly, treatment of a series of 10 individual CD73^{pos}/EGFR^{pos} cancer cell line types with bsAb CD73xEGFR demonstrated a positive linear dependence ($R^2=0.89$) between residual CD73 and EGFR cell surface-expression levels, whereas identical treatment with oleclumab failed to do so ($R^2=0.0003$) (figure 2H). Again, this indicated that on treatment with bsAb CD73xEGFR, cancer cell surface-exposed CD73 and EGFR are subject to antibody-mediated co-internalization.

bsAb CD73xEGFR potently inhibits the CD73 enzyme activity in an EGFR-directed manner

Treatment of various carcinomas with bsAb CD73xEGFR dose-dependently inhibited the CD73 enzyme activity (figure 3A, online supplemental file 3) and in this respect significantly outperformed oleclumab in three out of three cancer cell lines (group average; 71% vs 52%, respectively) (figure 3B) and in eight out of nine primary patient-derived carcinoma cells (group average; 55% vs 40%, respectively) (figure 3C). The respective IC₅₀ values of bsAb CD73xEGFR calculated for six cell lines ranged from 0.001 to 0.038 µg/mL, whereas those of oleclumab ranged from 0.005 to 0.563 µg/mL (online supplemental file 3). Additionally, inhibition of CD73 enzyme activity of H929 cancer cells by bsAb CD73xEGFR was dose-dependently decreased in presence of the EGFR-competing bsAb MockxEGFR (figure 3D). The CD73 enzyme activity of A549 EGFR-KO cancer cells was only marginally reduced on treatment with bsAb CD73xEGFR (figure 3E).

bsAb CD73xEGFR overcomes ADO-mediated suppression of T-cell proliferation

When activated CFSE-labeled T cells were subjected to AMP, which is locally enzymatically converted to ADO

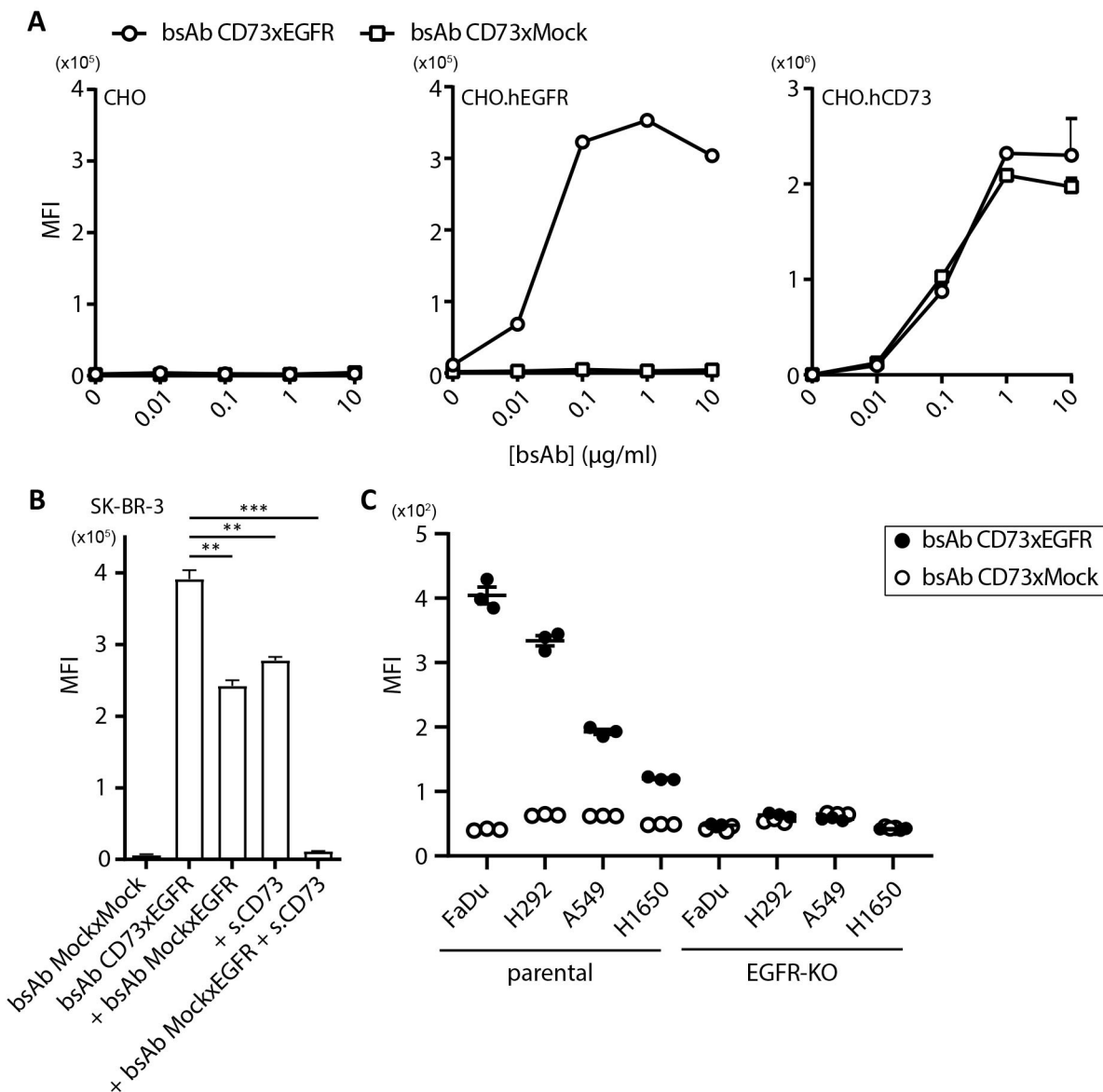


Figure 1 bsAb CD73xEGFR has dual binding specificity for CD73 and EGFR. (A) Dose-dependent binding of bsAb CD73xEGFR and bsAb CD73xMock to CHO, CHO.hEGFR and CHO.hCD73, respectively. (B) Competitive binding assay in which bsAb CD73xEGFR (1 μg/mL) was pre-incubated with excess amounts of soluble human CD73 (s.hCD73), EGFR-competing bsAb MockxEGFR or a combination thereof and then evaluated for binding to SK-BR-3 cancer cells. (C) Binding of bsAb CD73xEGFR and bsAb CD73xMock (both 1 μg/mL) to parental cancer cells (FaDu, H292, A549, H1650) and corresponding EGFR-KO variants thereof. All experiments were analyzed by flow-cytometry. Graphs A–B (representative graphs): n=3 (two technical repeats), graph C: n=3 (three technical replicates). All graphs represent mean±SD. Statistical analysis in B was performed using one-way analysis of variance followed up by Tukey post hoc test (**p<0.01, ***p<0.001). bsAb, bispecific antibody; CHO, Chinese hamster ovary; KO, knockout; MFI, mean fluorescent intensity.

by CD73, their proliferation capacity was significantly repressed. Importantly, treatment with bsAb CD73xEGFR or oleclumab fully abrogated the ADO-mediated inhibition of T-cell proliferation, as can be appreciated from the successive dilution of the CFSE-dye (figure 4A). These results corroborated the increase in activated T-cell cluster size (figure 4B).

bsAb CD73xEGFR restores anticancer activity of ADO-suppressed cytotoxic T cells

When cytotoxic T cells were subjected to AMP and subsequently redirected to kill EpCAM-expressing cancer cells

using EpCAM-directed/CD3-agonistic bsAb BIS-1, induction of cancer cell death, evident from high caspase-3/8 activation levels in target cells, significantly dropped (figure 4C,D, online supplemental file 3). Importantly, treatment with bsAb CD73xEGFR dose-dependently restored the capacity of these ADO-suppressed T cells to eliminate cancer cells (figure 4E). These results corroborate ELISA data quantifying the restored capacity of cytotoxic T cells to secrete IFN-γ (figure 4F).

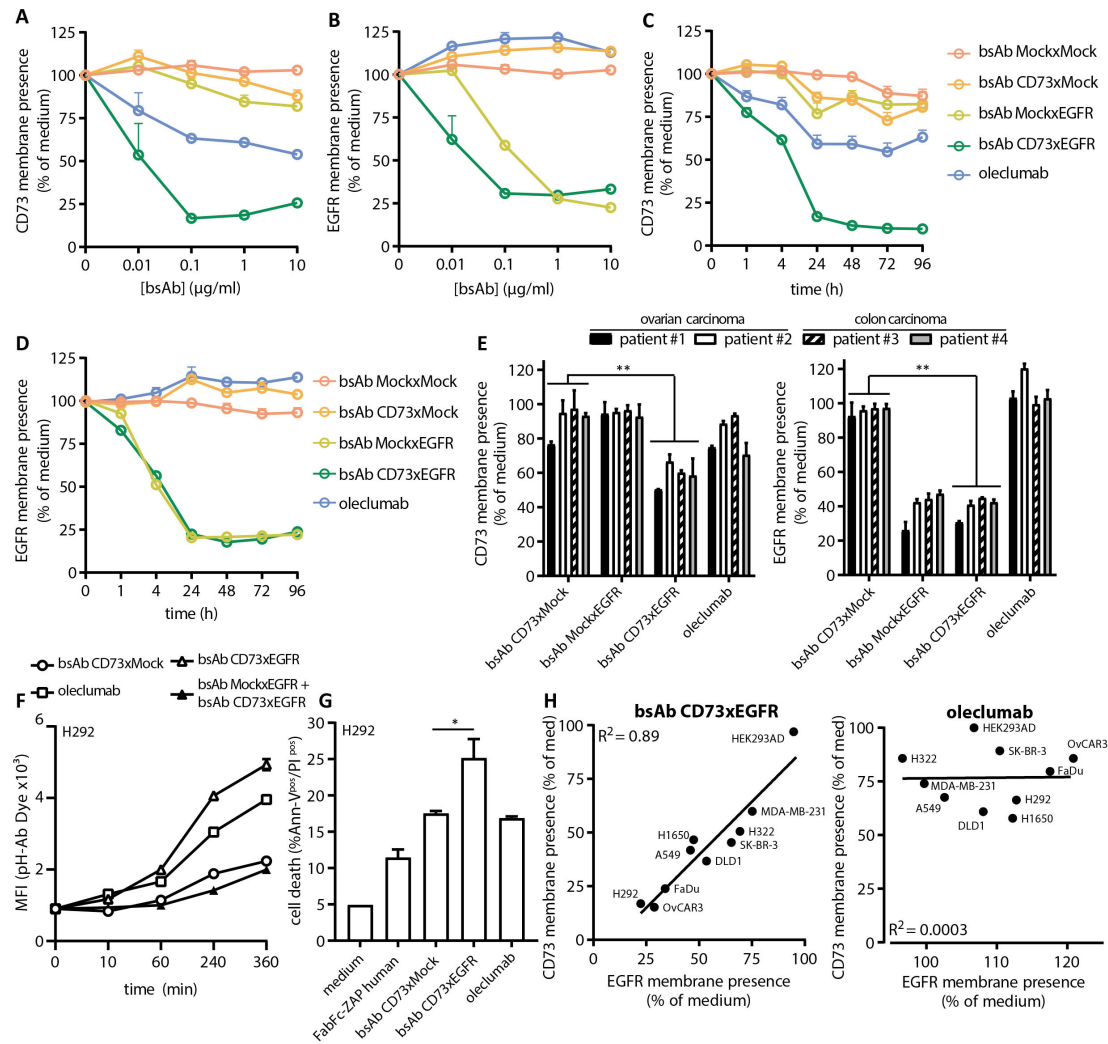


Figure 2 bsAb CD73xEGFR induces rapid co-internalization and subsequent prolonged displacement of both CD73 and EGFR from the cancer cell surface. Residual (A) CD73 and (B) EGFR membrane presence on H292 cells after treatment with bsAb CD73xEGFR or controls (0.01–10 μg/mL) for 24 hours. Residual (C) CD73 and (D) EGFR membrane presence on H292 cells after treatment with bsAb CD73xEGFR or controls (1 μg/mL) for 1, 4, 24, 48, 72 and 96 hours. (E) Residual CD73 and EGFR membrane presence after treatment of primary patient-derived ovarian and colon cancer cells with bsAb CD73xEGFR or controls (1 μg/mL) for 24 hours. (F) Mean fluorescent intensity (MFI) of H292 cells after incubation with bsAb CD73xEGFR or controls (1 μg/mL) labeled with pH-sensitive dye CypHer5E for 10, 60, 240 and 360 min. (G) Percentage of annexin-V^{pos}/PI^{pos} H292 cancer cells after incubation for 24 hours with bsAb CD73xEGFR or controls (1 μg/mL) in the presence of an anti-human IgG-Fab fragment labeled with a saprocin-based toxin. (H) Residual cell surface EGFR-expression levels plotted against residual cell surface CD73-expression levels of a panel of 10 cancer cell lines after treatment with bsAb CD73xEGFR or oleclumab (both 1 μg/mL) for 24 hours. All experiments were analyzed by flow-cytometry. Graphs A–D: n=4 (two technical replicates), graph E: n=1 (four technical replicates), graph F (representative graph): n=3 (two technical replicates), graph G: n=2 (three technical replicates), graph H: n=3 (two technical replicates). All graphs represent mean±SD. Statistical analysis in E (based on group-means) and G was performed using unpaired t-test (*p<0.05, **p<0.01). Linear regression was used to calculate the regression coefficient in graph H. bsAb, bispecific antibody.

bsAb CD73xEGFR increases the tumor-infiltrating capacity of leukocytes in immunocompetent mice

Subsequently, the apparent effect of *in vitro* treatment with bsAb CD73xEGFR on the anticancer activities of cytotoxic T cells was evaluated *in vivo* using BALB/c mice inoculated with CT26 cancer cells (in *in vitro* data CT26; online supplemental file 3). At 4, 7, 10, and 14 days after inoculation, animals were treated I.P. with 7.5 mg/kg bsAb CD73xEGFR, oleclumab, or controls (figure 5A). *In vivo* treatment with bsAb CD73xEGFR significantly reduced

tumor volume (65%) and tumor wet-weight (77%), thereby markedly outperforming oleclumab (31% reduction in tumor volume) (figure 5B,C, online supplemental file 3). Importantly, tumors procured from animals treated with bsAb CD73xEGFR showed increased infiltration of CD4^{pos} and CD8^{pos} lymphocytes and a decreased infiltration of FoxP3^{pos} lymphocytes (figure 5D–G, online supplemental file 3). Moreover, in these tumors an increased infiltration of F4/80^{pos} (total macrophage) and CD11c^{pos} (M1 macrophage) cells, and a decreased infiltration of CD206^{pos} (M2

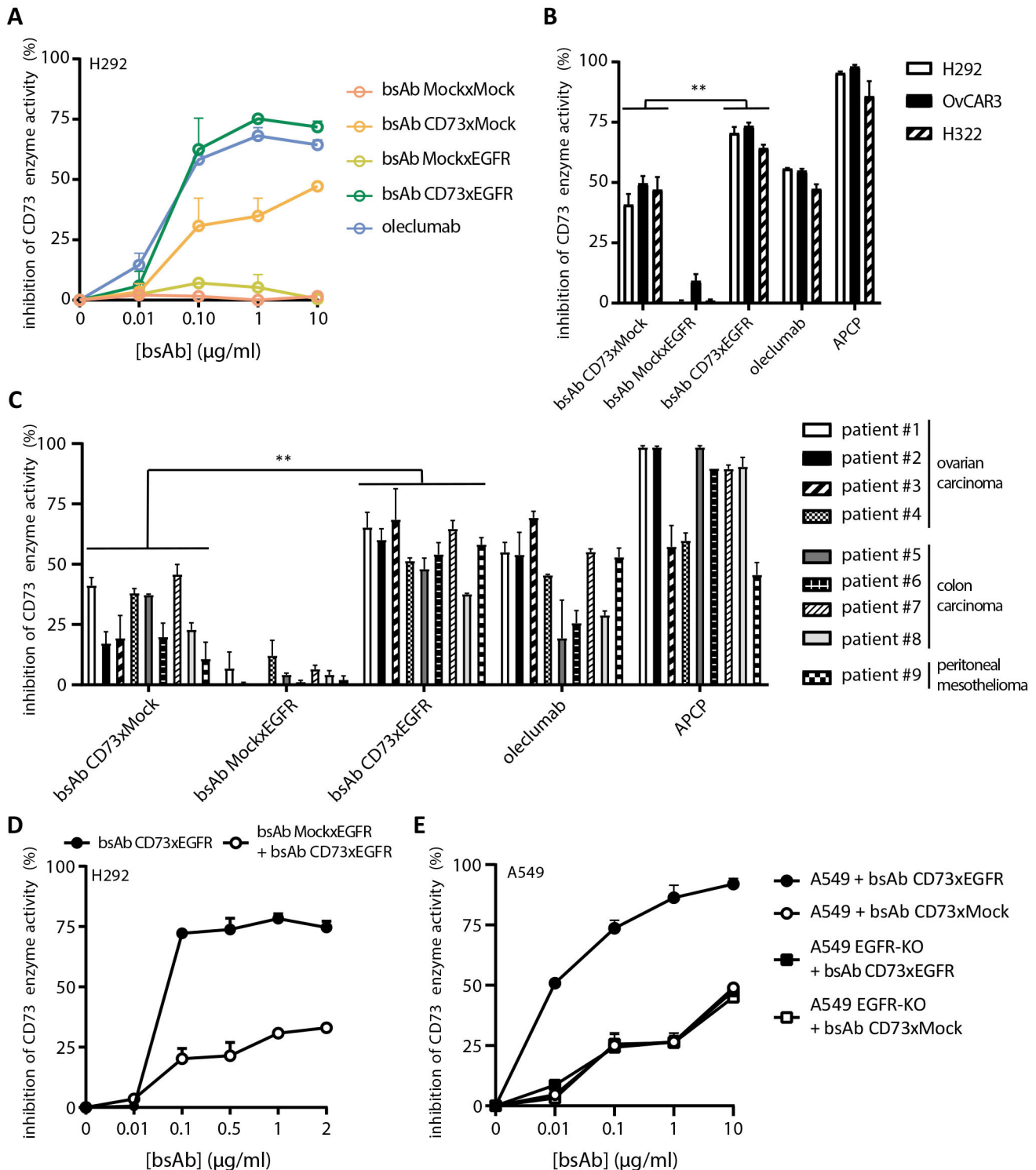


Figure 3 bsAb CD73xEGFR potently inhibits the enzyme activity of CD73 in an EGFR-directed manner. (A) Percentage of inhibition CD73 enzyme activity on H292 cells after treatment with bsAb CD73xEGFR or controls (0.01–10 $\mu\text{g/ml}$) for 24 hours. (B) Percentage of inhibition CD73 enzyme activity on H292, OvCAR3, and H322 cancer cell lines or on (C) primary patient-derived cancer cells after treatment with bsAb CD73xEGFR or controls (1 $\mu\text{g/ml}$) for 24 hours. (D) Competitive CD73 enzyme inhibition assay in which H292 cells were pretreated with excess amounts EGFR-competing bsAb MockxEGFR prior to incubation with bsAb CD73xEGFR (0.01–2 $\mu\text{g/ml}$). (E) Percentage of inhibition CD73 enzyme activity on A549 parental and EGFR-KO cells after treatment with bsAb CD73xEGFR or bsAb CD73xMock (both 1 $\mu\text{g/ml}$). CD73-mediated hydrolysis of AMP into adenosine was evaluated using a colorimetric malachite green-based inorganic phosphate assay. Graphs A–B: $n=4$ (two technical replicates), graph C: $n=1$ (four technical replicates), graph D–E: $n=3$ (two technical replicates). All graphs represent mean \pm SD. Statistical analysis in B and C was performed using unpaired t-test (based on group-means) (** $p < 0.01$). bsAb, bispecific antibody; KO, knockout.

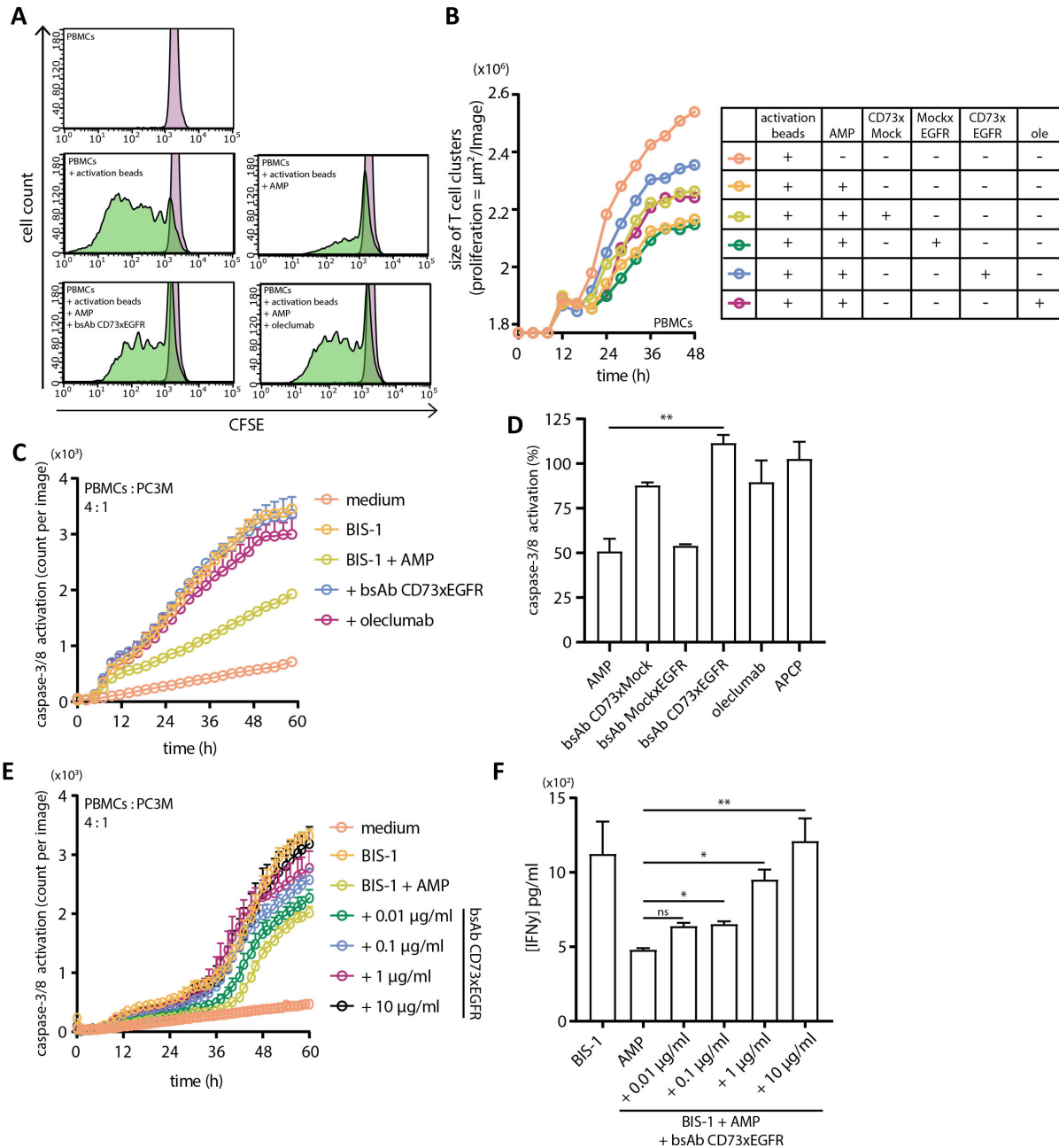


Figure 4 bsAb CD73xEGFR restores anticancer activities of ADO-suppressed T cells. (A) Cell count of activated CFSE-labeled PBMCs, cultured in medium supplemented with AMP, in the presence (or absence) of bsAb CD73xEGFR or controls (1 μ g/mL) at 37°C for 5 days. Subsequently, CFSE-dye dilution was evaluated by flow-cytometry. Both unstimulated (purple) and ADO-inhibited T cells are indicated by bright single peaks on the right side of the histogram. The discrete successive peaks (green) in the histograms represent successive generations of live T cells due to dilution of cytoplasmic CFSE-dye. (B) Similar, the size of proliferating T cells clusters ($\mu\text{m}^2/\text{image}$) was quantified using live cell imagine by taking pictures at 10 \times magnification at 37°C every 1.5 hours for 2 days. (C) Caspase-3/8 activation (apoptotic cancer cell death) in PC3M cancer cells, killed by redirected PBMCs using BIS-1 (bsAb CD3xEPcAM) in an effector (E) to target (T) cell ratio of 4:1. Importantly, PBMCs were incubated with (or without) AMP, in the presence, or absence, of bsAb CD73xEGFR, oleclumab or (D) controls (all 1 μ g/mL). Caspase-3/8 activation (count per image) was evaluated using live cell imagine technology by taking pictures at 10 \times magnification at 37°C every 1.5 hours for 2.5 days. (E) Similar, PBMCs were incubated with increasing amounts of bsAb CD73xEGFR (0.01–10 μ g/mL), subjected to AMP, redirected in order to kill PC3M cancer cells and analyzed as indicated above. (F) Interferon- γ levels in culture supernatant of E were measured by ELISA. Graph A (representative graph): n=3 (two technical replicates), graph B (representative graph): n=3 (four technical replicates), graph C (representative graph): n=3 (four technical replicates), graph D: n=3 (four technical replicates), graph E (representative graph): n=3 (four technical replicates), graph F: n=3 (four technical replicates). All graphs represent mean \pm SD. Ole=oleclumab in graph B. Statistical analysis in D and F was performed using one-way analysis of variance followed up by Tukey post hoc test (*p<0.05, **p<0.01). ADO, adenosine; bsAb, bispecific antibody; IFN, interferon; PBMCs, peripheral blood mononuclear cells; EpCAM, epithelial cell adhesion molecule; CFSE; carboxyfluorescein succinimidyl ester.

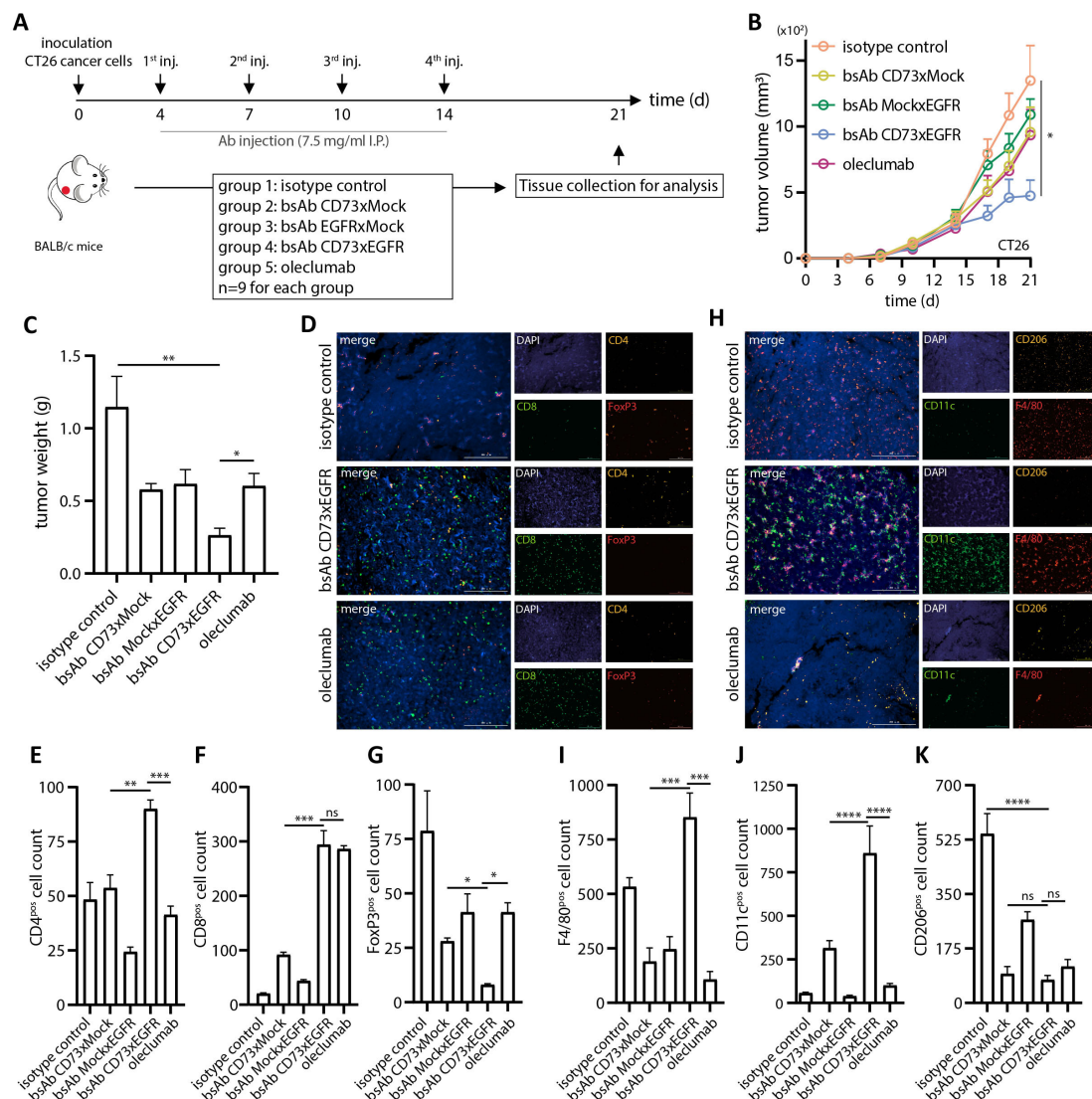


Figure 5 bsAb CD73xEGFR markedly enhanced the intratumoral presence of CD8^{pos} T cells and M1 macrophages in immunocompetent mice. (A) Immunocompetent BALB/c mice were inoculated with murine CT26 colon carcinoma cells subcutaneous into the flank and injected I.P. with bsAb CD73xEGFR (7.5 mg/kg) or controls on days 4, 7, 10, and 14. Tumor and organs were harvested for analysis 21 days post tumor injection. (B) Mean tumor volume and (C) wet tumor weight of each nine animals per group. (D) Representative images of multiplexed immunofluorescence staining and quantification for (E) CD4, (F) CD8, (G) and FoxP3 in tumor sections derived from isotype, bsAb CD73xEGFR or oleclumab treated mice. (H) Representative images of multiplexed immunofluorescence staining and quantification for (I) F4/80, (J) CD11c and (K) CD206 in tumor sections derived from isotype, bsAb CD73xEGFR or oleclumab treated mice. All graphs represent mean±SD. Scale bar in D and H=200µm. Statistical analysis in B (at 21 days), C, E–G, and I–K was performed using one-way analysis of variance followed up by Tukey post hoc test (* $p < 0.05$, ** $p < 0.01$, *** $p < 0.001$, **** $p < 0.0001$, ns=not significant). bsAb, bispecific antibody; I.P., intraperitoneal.

macrophage) cells was observed (figure 5H–K, online supplemental file 3). In contrast, tumors procured from animals treated with oleclumab only demonstrated an increased infiltration with CD8^{pos} lymphocytes and a decreased infiltration of total and M2 macrophages. Importantly, animals treated with bsAb CD73xEGFR appeared to show no signs of systemic toxicity in vital organs (online supplemental file 3).

bsAb CD73xEGFR inhibits proliferative and migratory capacity of cancer cells in vitro

Both enzymatic and non-enzymatic attributes of CD73 overexpression were reported to be implicated in enhancement of cancer cell proliferative/migratory capacity and resistance to chemo/radiotherapy.¹² In this respect, it is noteworthy that treatment with bsAb CD73xEGFR decreased the proliferative capacity of carcinoma cell line types (four out of four) by ~40% (figure 6A,B, online supplemental file 3). Additionally, treatment with bsAb CD73xEGFR significantly reduced the colony forming capacity of cancer cells both in number and

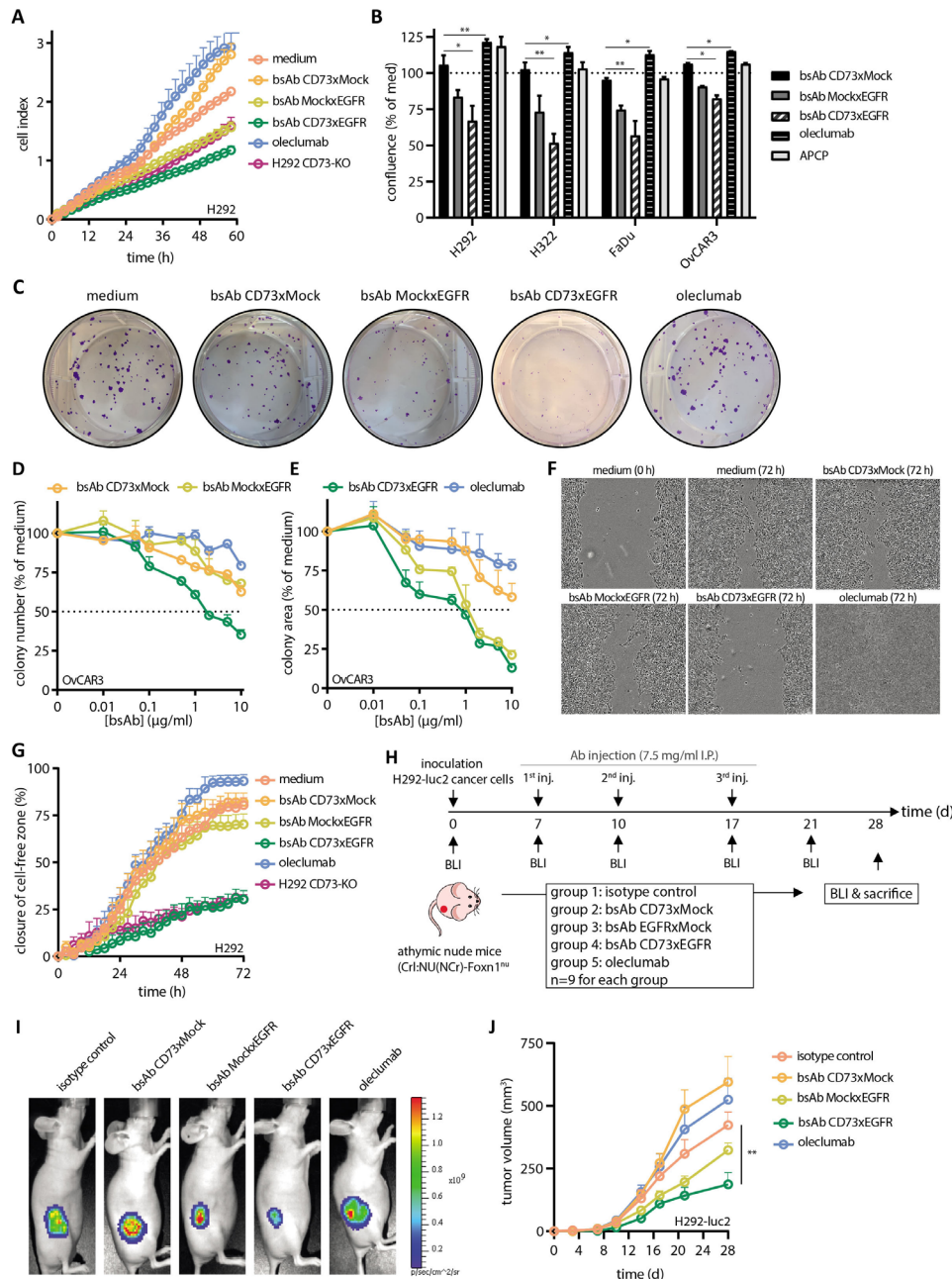


Figure 6 bsAb CD73xEGFR inhibits the proliferative and migratory capacity of cancer cells. (A) Proliferation assay in which H292 and corresponding CD73-KO cancer cells were incubated with bsAb CD73xEGFR or controls (1 $\mu\text{g/ml}$) and then evaluated using the RTCA xCELLigence instrument. Readout is indicated as cell-index, which is an arbitrary unit for attachment of adherent cells and cell proliferation measured at 37°C every 15 min. (B) Proliferation assay in which a panel of cell lines (H292, H322, FaDu, and OvCAR3) was incubated with bsAb CD73xEGFR or controls (1 $\mu\text{g/ml}$). The percentage of cell confluence was evaluated after 72 hours. (C) Representative images of H292 cell colonies after treatment with bsAb CD73xEGFR (1 $\mu\text{g/ml}$) or indicated controls at 37°C for 14 days. (D, E) Percentage of OvCAR3 cell colonies after treatment with bsAb CD73xEGFR or controls (0.01–10 $\mu\text{g/ml}$) at 37°C for 14 days. Subsequently, number and area of OvCAR3 cell colonies were calculated using ImageJ software. (F) Representative images of H292 cells, seeded in a culture plate equipped with a stopper, which enabled the formation of a cell-free detection zone, and incubated with bsAb CD73xEGFR or controls (1 $\mu\text{g/ml}$) at 37°C for 72 hours. (G) Similar, closure of cell-free detection zone (migration) evaluated over time using live cell imaging technology by taking pictures at 4 \times magnification at 37°C every 0.5 hours for 3 days. (H) Athymic nude mice (CrI:NU(NCr)-Foxn1^{nu}) were inoculated subcutaneous in the flank with human H292-luc2 non-small lung cancer cells and injected I.P. with bsAb CD73xEGFR or controls (7.5 mg/kg) on days 7, 10, and 17. (I) Representative bioluminescent images of bsAb CD73xEGFR or control treated mice on day 28 post tumor injection. (J) Mean tumor volume (mm^3) of each nine animals per group determined by caliper measurements. Graph A–B: n=3 (two technical replicates), Graph D–E: n=3 (two technical replicates), graph G: n=3 (two technical replicates). All graphs represent mean \pm SD. Statistical analysis in B and in J (at 28 days) was performed using one-way analysis of variance followed up by Tukey post hoc test (* p <0.05, ** p <0.01). APCP, adenosine 5'-(α , β -methylene)diphosphate; bsAb, bispecific antibody; I.P., intraperitoneal; KO, knockout.

size (figure 6C–E). In this respect, IC_{50} values calculated for bsAb CD73xEGFR ranged from 0.16 to 0.65 $\mu\text{g}/\text{mL}$, which was superior compared with oleclumab (IC_{50} 9.38–24.33 $\mu\text{g}/\text{mL}$) in three out of three cell lines tested (online supplemental file 3). Representative light-microscopic pictures shown in figure 6F indicate that treatment of cancer cells with bsAb CD73xEGFR almost fully abrogated their migratory capacity. These results corroborate the observed delayed closure of the cell-free zone over time on treatment with bsAb CD73xEGFR (figure 6G).

Unexpectedly, *in vitro* treatment of various carcinoma cell line types with oleclumab (or small-molecule CD73-inhibitor APCP) appeared to rather promote than inhibit cancer cell growth (figure 6B). Moreover, treatment with oleclumab enhanced the migration capacity of cancer cells by ~20% (figure 6G). These results may be explained by the fact that *in vitro* treatment with oleclumab enhanced (both total and phosphorylated) EGFR and HER2 levels in these cancer cells (online supplemental file 3). Of note, oleclumab-induced upregulation of cell-surface expressed EGFR is also apparent in figure 2H in 8 out of 10 cell lines evaluated.

bsAb CD73xEGFR inhibits the proliferative capacity of xenografted cancer cells in immunodeficient mice

Subsequently, the apparent opposing effect of *in vitro* treatment with bsAb CD73xEGFR versus oleclumab treatment on the proliferative capacity of cancer cells was evaluated *in vivo* using athymic nude mice inoculated with H292-Luc2 cells. At 7, 10, and 17 days after inoculation, animals were treated I.P. with 7.5 mg/mL bsAb CD73xEGFR, oleclumab, or controls (figure 6H). Compared with treatment with isotype control, *in vivo* treatment with bsAb CD73xEGFR inhibited tumor growth by 56% (figure 6I,J, online supplemental file 3). In comparison, the volume of tumors that developed in animals treated with oleclumab or bsAb CD73xMock increased by 24% and 40%, respectively.

bsAb CD73xEGFR sensitizes cancer cells towards treatment with chemotherapeutic agents and ionizing radiation

In vitro co-treatment with bsAb CD73xEGFR sensitized cancer cells towards the cytotoxic activity of cisplatin, doxorubicin, taxol, and 5FU by ~1-fold, 0.45-fold, 0.74-fold, and 0.4-fold, respectively (figure 7A,B, online supplemental file 3). In contrast, treatment with oleclumab enhanced resistance of cancer cells towards cisplatin, doxorubicin, and 5FU by ~2-fold, 1.8-fold, and 1.44-fold, respectively.

Similarly, co-treatment with bsAb CD73xEGFR enhanced sensitivity of cancer cells towards cytotoxicity induced by ionizing radiation (figure 7C). In this respect, IC_{50} values calculated for bsAb CD73xEGFR treatment decreased from 1.35 Gy to 0.536 Gy (figure 7E). In contrast, identical treatment with oleclumab enhanced resistance towards ionizing radiation up to 39% at 2 Gy (figure 7C), whereas calculated IC_{50} values increased from 1.35 Gy to 3.77 Gy (figure 7E). Importantly, treatment of

CD73-KO cancer cells with oleclumab did not change their resistance towards ionizing radiation (figure 7D).

DISCUSSION

Antagonistic CD73 antibodies like oleclumab⁴ appear useful to overcome the inhibitory activity of the CD73/ADO immune checkpoint in a broad variety of cancer types. Currently, several multicenter trials are ongoing to evaluate the clinical potential of oleclumab as an immune checkpoint inhibitor in patients with advanced solid malignancies, including various carcinomas. Unfortunately, recent midterm clinical trial reports indicate that, as a single treatment modality, the efficacy of oleclumab remains modest at best.^{13–16} Possibly, monospecific antagonistic CD73 antibodies like oleclumab suffer from “on-target/off-tumor” binding to CD73 molecules present on normal cells,⁵ which limits CD73-inhibitory activity at the tumor site(s).

Here, we report on the construction and preclinical evaluation of bsAb CD73xEGFR that was engineered to inhibit cancer cell surface-expressed CD73 in an EGFR-directed manner. We selected EGFR for this purpose as it is a well-established tumor-associated cell surface target antigen that is frequently mutated and/or overexpressed by various difficult-to-treat solid malignancies.^{17,18} Moreover, many malignancies were shown to selectively co-overexpress CD73 and EGFR.^{19–21} BsAb CD73xEGFR is equipped with two identical scFv antibody fragments derived from oleclumab and two identical EGFR-directed nanobodies. Of note, these antibody domains bind to their respective human—and mouse orthologues with similar affinities. This strategy allows for preclinical evaluation of bsAb CD73xEGFR in both human and murine tumor model systems. To exclude antibody-dependent cellular cytotoxicity (ADCC)-mediated antitumor effects during such evaluation, we equipped bsAb CD73xEGFR with an IgG2-silent Fc domain with nullified effector function.²²

Importantly, compared with oleclumab, bsAb CD73xEGFR showed superior antagonistic activity towards cancer cells that co-overexpress CD73 and EGFR. This superiority is most likely attributable to the enhanced avidity associated with the tetravalent format of bsAb CD73xEGFR. Previously, we reported on similar attributes for tetravalent bsAbs that were designed to block immune checkpoints PD-L1^{23,24} and CD47^{25,26} in a more tumor-selective manner. More recently, we reported on tetravalent bsAb CD73xEpCAM, which allowed to potently inhibit CD73 exposed on carcinoma-derived exosomes, whereas oleclumab showed no or very limited capacity to do so.⁹

Intriguingly, *in vitro* treatment of CD73^{pos}/EGFR^{pos} cancer cells, both various cell lines and primary patient-derived cancer cell types, with bsAb CD73xEGFR induced the rapid internalization of bsAb/antigen complexes, resulting in the prolonged and concurrent displacement of CD73 and EGFR from the cancer cell surface for up

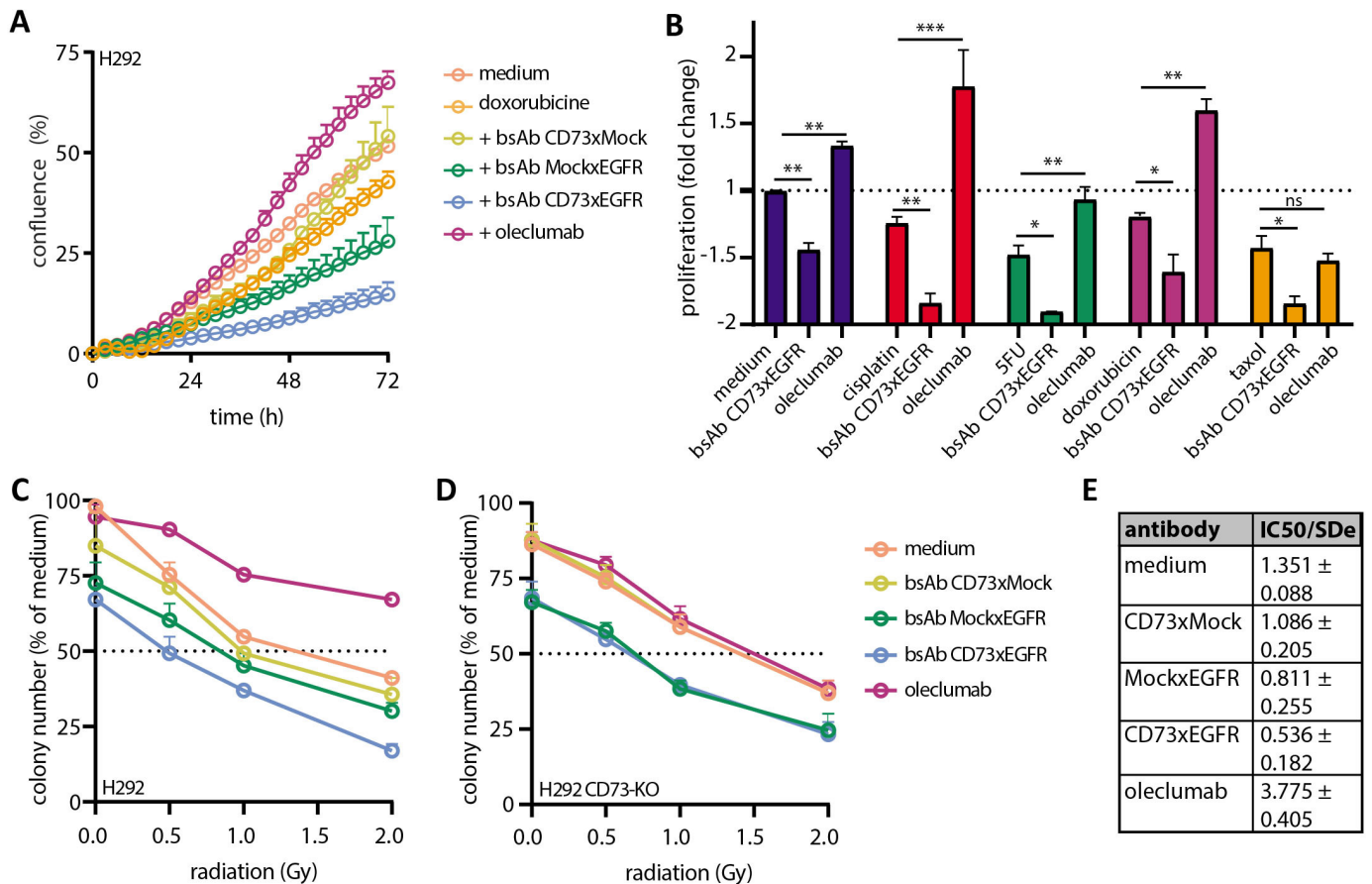


Figure 7 bsAb CD73xEGFR sensitizes cancer cells towards chemotherapeutic agents and radiation. Cell confluence of H292 cancer cells treated (or not) with bsAb CD73xEGFR (1 μ g/mL) or controls in the presence (or absence) of (A/B) doxorubicin (50 nM), (B) cisplatin (1 μ g/mL), taxol (50 nM) or 5FU (50 μ g/mL) and then evaluated using live cell imaging by taking pictures at 4 \times magnification every 6 hours at 37 $^{\circ}$ C for 6 days. (C) Percentage of H292 or (D) corresponding CD73-KO cell colonies after treatment with bsAb CD73xEGFR (1 μ g/mL) or controls, irradiated (0.5, 1, 1.5, and 2 Gy) and then incubated at 37 $^{\circ}$ C for 14 days. Cell colonies were calculated using ImageJ software. (E) IC₅₀ values (Gy) calculated for graph C. All graphs: n=3 (two technical replicates). All graphs represent mean \pm SD. Statistical analysis in B was performed using unpaired t-test (*p<0.05, **p<0.01, ***p<0.001). bsAb, bispecific antibody; KO, knockout.

to 96 hours. Of note, the internalization of oleclumab (labeled with CypHer5E) is higher than that of bsAb CD73xMock. This may be explained by the fact that CypHer5E NHS-Ester-based labeling may be more efficient for a conventional antibody like oleclumab than for the bispecific taFv-Fc format of our bsAbs. Although not investigated here, such difference may result in higher dye-to-antibody ratio for oleclumab.

The bsAb CD73xEGFR-induced internalization of cancer cell surface-exposed CD73 resulted in a similarly prolonged incapacity of these cancer cells to convert extracellular AMP to ADO. Importantly, in vitro treatment of ADO-suppressed cytotoxic T cells with bsAb CD73xEGFR potentially reinvigorated their anticancer activities. Moreover, compared with controls, treatment with bsAb CD73xEGFR of immunocompetent BALB/c mice (7.5 mg/kg) inoculated with syngeneic CT26 colorectal carcinoma cells, resulted in an average reduction of 65% in tumor size development, whereas identical treatment with oleclumab reduced tumor size by only 31%. Importantly, the in vivo application of bsAb CD73xEGFR

increased the presence of tumor-infiltrating CD4^{pos} T cells,—CD8^{pos} T cells, and—macrophages by 38%, 52%, and 82%, respectively. These results appear favorable compared with those reported by Hay *et al*¹ using essentially the same mouse tumor model in which treatment with oleclumab (at 10 mg/kg) resulted in a reduction in tumor size of 57% (at 16 days) and an increase in tumor-infiltrating CD4^{pos} T cells,—CD8^{pos} T cells, and—macrophages by only 15%, 25%, and 20%, respectively. Of note, our in vitro data confirms that bsAb CD73xEGFR has potent capacity to inhibit the enzyme activity of mCD73 on CT26 cells. However, treatment of CT26 cancer cells with bsAb CD73xEGFR does not induce co-internalization of mCD73 and mEGFR. The reason for this difference between human and murine cancer cells remains to be determined.

Several reports indicated that overexpression of CD73 is implicated in the enhancement of various oncogenic attributes of cancer cells, including increased cell proliferation and migration capacity.¹² To evaluate whether bsAb CD73xEGFR has capacity to counteract the oncogenic



attributes of CD73 overexpression, we treated immunodeficient mice inoculated with EGFR-overexpressing H292-luc tumor cells with bsAb CD73xEGFR and assessed its treatment effect on tumor outgrowth. Indeed, treatment with bsAb CD73xEGFR potently reduced the size of xenografted tumors. In contrast, and rather unexpectedly, identical treatment with oleclumab (or bsAb CD73xMock) appeared to enhance the growth capacity of xenografted H292-luc carcinoma cells. Intriguingly, *in vitro* treatment of H292-luc cells with oleclumab also resulted in enhancement of tumor growth, which coincided with enhanced expression—and phosphorylation levels of oncogenic proteins EGFR and HER2 in these cancer cells. In this respect, our observations appear to contradict with those mentioned in some previous reports.^{12 27 28} Apparently, apart from its ADO-producing activity, cancer cell-exposed CD73 appears to serve as a signaling transduction molecule that can deliver opposing intracellular signals. Because CD73 is linked to the cell surface by a glycosylphosphatidylinositol (GPI) anchor, the transduction of such signals is probably indirectly mediated by a lateral interaction with juxtaposed transmembrane molecules.²⁹ Depending on the particular membrane context, CD73 signaling may thus be coupled to either their tyrosine kinase or phosphatase activities (or possibly both). Similarly, it has been previously reported that CD73 present on CD8^{pos} T cells can act as a co-stimulatory signal by laterally interacting with receptor-linked protein tyrosine phosphatase CD45RC.³⁰ We speculate that cancer cell-expressed CD73 may have analogous capacity to modulate oncogenic activities of EGFR and HER2 in a direct or indirect manner. The underlying mechanism by which oleclumab treatment promoted tumor growth and enhanced expression and phosphorylation levels of EGFR and HER2 in our model systems remains to be elucidated by follow-up studies.

Previously, it was reported that patients with cancer treated with chemotherapeutic agents, such as carboplatin, gemcitabine, and paclitaxel, show enhanced CD73 expression levels on cancer cells,³¹ which correlate with adopting a multidrug-resistance phenotype.^{32 33} To evaluate whether bsAb CD73xEGFR has capacity to counteract multidrug-resistance, we treated cancer cells *in vitro* with bsAb CD73xEGFR and assessed its treatment effect on the sensitivity of these cells towards cytotoxicity induced by various chemotherapeutic agents. In this respect, it is encouraging that bsAb CD73xEGFR sensitized cancer cells towards the cytotoxicity of cisplatin, doxorubicin, taxol and 5FU, respectively. Surprisingly, combined treatment of cancer cells with bsAb CD73xMock and bsAb MockxEGFR or oleclumab and cetuximab did not have similar effects as treatment with bsAb CD73xEGFR alone. This suggests that bsAb CD73xEGFR sensitizes cancer cells towards the cytotoxicity of chemotherapeutic agents through the concurrent removal of (juxtaposed) CD73 and EGFR molecules from the cell surface.

Analogously, *in vitro* treatment with bsAb CD73xEGFR enhanced the sensitivity of H292 non-small-lung cancer

cells towards radiation-induced cytotoxicity up to ~40%. In contrast, identical treatment with oleclumab reduced sensitivity of these cancer cells towards ionizing radiation and increased the IC₅₀ value from 1.35 Gy to 3.77 Gy. The latter observation appears to corroborate with those of Dietrich *et al.*³⁴ who reported that inhibition of the enzyme activity of CD73 by small-molecule CD73-inhibitor APCP promoted the proliferative capacity of irradiated cancer cells, thereby enhancing their radiation-resistance, due to the absence of (locally) accumulated ADO. This suggests that CD73-produced ADO potentiates radiation-induced cell death in certain cancer types. Of note, in our study, treatment of H292 cancer cells with bsAb CD73xMock did not increase their resistance to radiation. This may be due to the fact that, compared with oleclumab, bsAb CD73xMock has a somewhat lower capacity to inhibit the enzyme activity of CD73. Whether the observed oleclumab-induced enhancement to radiation also applies to other cancer cell lines/types remains to be evaluated in follow-up studies.

In conclusion, bsAb CD73xEGFR appears to be a promising approach to overcome the inhibitory activity of the CD73/ADO immune checkpoint in a broad variety of cancer types. In particular, it allows to inhibit the CD73 enzyme activity in a more tumor-selective manner, while simultaneously counteracting pro-oncogenic activities of CD73 and EGFR. Therefore, bsAb CD73xEGFR may be of significant clinical potential for various forms of difficult-to-treat solid cancer types.

Author affiliations

¹Department of Surgery, Laboratory for Translational Surgical Oncology, University of Groningen, University Medical Center Groningen, Groningen, The Netherlands

²Department of Urology, Guangdong Second Provincial General Hospital, Guangzhou, Guangdong, China

³Faculty of Medical Science and Integrated Chinese and Western Medicine Postdoctoral research station, Jinan University, Guangzhou, Guangdong, China

⁴Affiliated Cancer Hospital of Shantou University Medical College, Shantou, Guangdong, China

⁵Department of General Surgery, Jinan University First Affiliated Hospital, Institute of Precision Cancer Medicine and Pathology, School of Medicine, Jinan University, Guangzhou, Guangdong, China

⁶Minister of Education Key Laboratory of Tumor Molecular Biology, Jinan University, Guangzhou, Guangdong, China

Contributors Conceptualization: EMP and WH. Methodology: EMP, DFS, HZ, and WH. Investigation: EMP, DFS, XK, XX, IB, APwV, and MAJMH. Visualization: EMP. Funding acquisition: WH. Writing (original text): EMP and WH. Writing (review and editing): All authors. Guarantor: WH.

Funding This work was supported by the Dutch Cancer Society (project numbers 11464 and 6986, to WH).

Competing interests No, there are no competing interests.

Patient consent for publication Not applicable.

Provenance and peer review Not commissioned; externally peer reviewed.

Data availability statement All data relevant to the study are included in the article or uploaded as supplementary information.

Supplemental material This content has been supplied by the author(s). It has not been vetted by BMJ Publishing Group Limited (BMJ) and may not have been peer-reviewed. Any opinions or recommendations discussed are solely those of the author(s) and are not endorsed by BMJ. BMJ disclaims all liability and responsibility arising from any reliance placed on the content. Where the content

includes any translated material, BMJ does not warrant the accuracy and reliability of the translations (including but not limited to local regulations, clinical guidelines, terminology, drug names and drug dosages), and is not responsible for any error and/or omissions arising from translation and adaptation or otherwise.

Open access This is an open access article distributed in accordance with the Creative Commons Attribution Non Commercial (CC BY-NC 4.0) license, which permits others to distribute, remix, adapt, build upon this work non-commercially, and license their derivative works on different terms, provided the original work is properly cited, appropriate credit is given, any changes made indicated, and the use is non-commercial. See <http://creativecommons.org/licenses/by-nc/4.0/>.

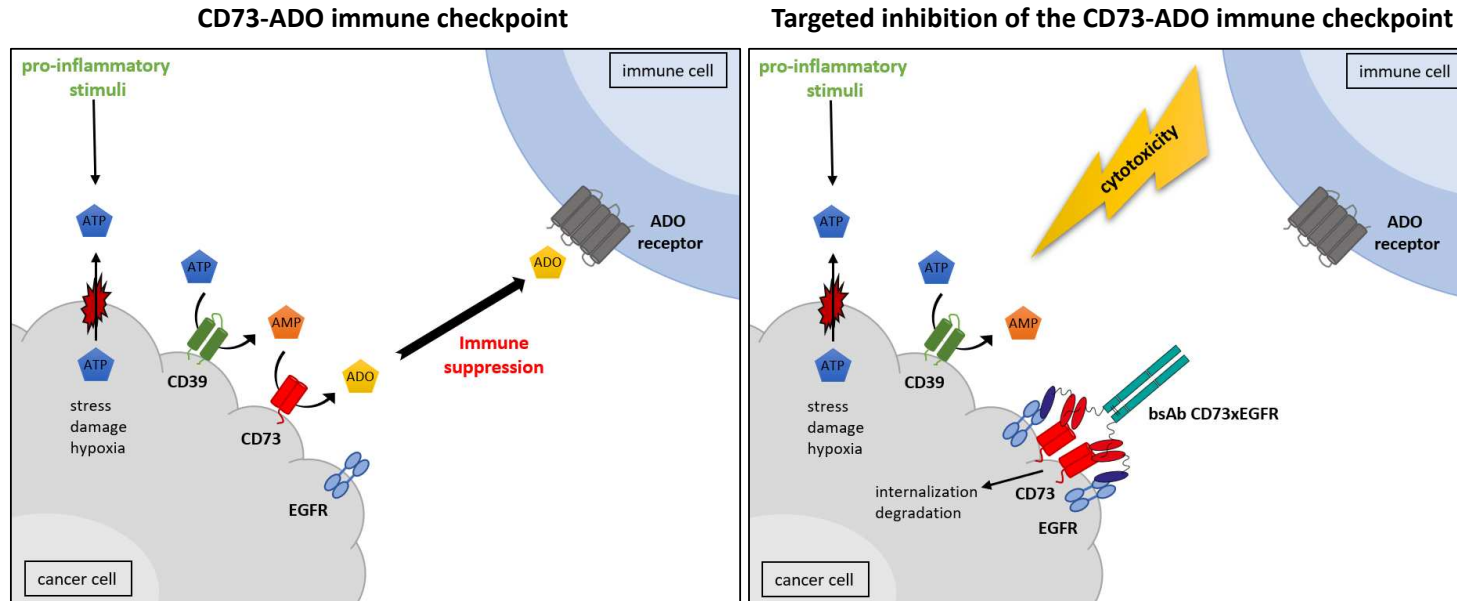
ORCID iDs

Emily Maria Ploeg <http://orcid.org/0000-0002-0735-2020>
 Douwe Freerk Samplonius <http://orcid.org/0000-0002-0613-7150>
 Xiurong Ke <http://orcid.org/0000-0001-8982-0950>
 Mark Alexander Johannes Martinus Hendriks <http://orcid.org/0000-0001-7276-4622>
 Isabel Britsch <http://orcid.org/0000-0003-4772-9889>
 Anne Paulien van Wijngaarden <http://orcid.org/0000-0002-8221-1180>
 Hao Zhang <http://orcid.org/0000-0002-2860-5912>
 Wijnand Helfrich <http://orcid.org/0000-0001-7004-3995>

REFERENCES

- Allard D, Allard B, Gaudreau PO, *et al*. Cd73-adenosine: a next-generation target in Immuno-oncology. *Immunotherapy* 2016;8:145–63.
- Allard B, Allard D, Buisseret L, *et al*. The adenosine pathway in Immuno-oncology. *Nat Rev Clin Oncol* 2020;17:611–29.
- Antonoli L, Blandizzi C, Malavasi F, *et al*. Anti-Cd73 Immunotherapy: A viable way to Reprogram the tumor Microenvironment. *Oncoimmunology* 2016;5:e1216292.
- Hay CM, Sult E, Huang Q, *et al*. Targeting Cd73 in the tumor Microenvironment with Medi9447. *Oncoimmunology* 2016;5:e1208875.
- Keizer RJ, Huitema ADR, Schellens JHM, *et al*. Clinical pharmacokinetics of therapeutic Monoclonal antibodies. *Clin Pharmacokinet* 2010;49:493–507.
- Liu B, Song S, Setroikromo R, *et al*. n.d. CX Chemokine receptor 7 contributes to survival of KRAS-mutant non-small cell lung cancer upon loss of Epidermal growth factor receptor. *Cancers*;11:455.
- Zhang J-P, Li X-L, Neises A, *et al*. Different effects of sgRNA length on CRISPR-mediated gene knockout efficiency. *Sci Rep* 2016;6:28566.
- Rossotti MA, Henry KA, van Faassen H, *et al*. Camelid single-domain antibodies raised by DNA immunization are potent inhibitors of EGFR signaling. *Biochem J* 2019;476:39–50.
- Ploeg EM, Ke X, Britsch I, *et al*. Bispecific antibody Cd73Xepcam selectively inhibits the adenosine-mediated immunosuppressive activity of carcinoma-derived extracellular Vesicles. *Cancer Lett* 2021;521:109–18.
- Xiong X, Ke X, Wang L, *et al*. Neoantigen-based cancer vaccination using Chimeric RNA-loaded Dendritic cell-derived extracellular Vesicles. *J Extracell Vesicles* 2022;11:e12243.
- Brinkmann U, Kontermann RE. The making of Bispecific antibodies. *MAbs* 2017;9:182–212.
- wei GZ, Dong K, zhong ZH. The roles of Cd73 in cancer. *Biomed Res Int* 2014;2014:460654.
- Kondo S, Iwasa S, Koyama T, *et al*. Safety, tolerability, pharmacokinetics, and Antitumour activity of Oleclumab in Japanese patients with advanced solid malignancies: a phase I, open-label study. *Int J Clin Oncol* 2022;27:1795–804.
- Mirza M, Henriksen JR, Maenpaa J, *et al*. 1195 Results of NSGO-OV-UMB1/ENGOT-OV30 study: a phase II study of durvalumab and oleclumab in patients with relapsed ovarian cancer (OC). ESGO SoA 2021 Conference Abstracts; October 2021
- Somaiah N, Livingston JAA, Ravi V, *et al*. A phase II multi-arm study to test the efficacy of Oleclumab and Durvalumab in specific sarcoma subtypes. *JCO* 2022;40:TPS11594. 10.1200/JCO.2022.40.16_suppl.TPS11594 Available: https://doi.org/10.1200/JCO.2022.40.16_suppl.TPS11594
- Overman MJ, LoRusso P, Strickler JH, *et al*. Safety, efficacy and pharmacodynamics (PD) of Medi9447 (Oleclumab) alone or in combination with Durvalumab in advanced colorectal cancer (CRC) or Pancreatic cancer (Panc). *JCO* 2018;36:4123. 10.1200/JCO.2018.36.15_suppl.4123 Available: https://doi.org/10.1200/JCO.2018.36.15_suppl.4123
- Selvaggi G, Novello S, Torri V, *et al*. Epidermal growth factor receptor overexpression correlates with a poor prognosis in completely Resected non-small-cell lung cancer. *Ann Oncol* 2004;15:28–32.
- Yoshida T, Okamoto I, Okabe T, *et al*. n.d. Matuzumab and Cetuximab activate the Epidermal growth factor receptor but fail to trigger downstream signaling by AKT or Erk. *Int J Cancer*;122:1530–8.
- Zhi X, Wang Y, Yu J, *et al*. Potential Prognostic biomarker Cd73 regulates Epidermal growth factor receptor expression in human breast cancer. *IUBMB Life* 2012;64:911–20.
- Griesing S, Liao BC, Yang JCH. Cd73 is regulated by the EGFR-ERK signaling pathway in non-small cell lung cancer. *Anticancer Res* 2021;41:1231–42.
- Tu E, McGlinchey K, Wang J, *et al*. Anti-PD-L1 and anti-Cd73 combination therapy promotes T cell response to EGFR-Mutated NSCLC. *JCI Insight* 2022;7:e142843.
- Vafa O, Gilliland GL, Brezski RJ, *et al*. An engineered FC variant of an IgG eliminates all immune Effector functions via structural perturbations. *Methods* 2014;65:114–26.
- Koopmans I, Hendriks D, Samplonius DF, *et al*. A novel Bispecific antibody for EGFR-directed blockade of the PD-1/PD-L1 immune Checkpoint. *Oncoimmunology* 2018;7:e1466016.
- Koopmans I, Hendriks M, van Ginkel RJ, *et al*. Bispecific antibody approach for improved Melanoma-selective PD-L1 immune Checkpoint blockade. *J Invest Dermatol* 2019;139:2343–51.
- Hendriks MAJM, Ploeg EM, Koopmans I, *et al*. “Bispecific antibody approach for EGFR-directed blockade of the Cd47-SIRPα “don’t eat me” immune Checkpoint promotes neutrophil-mediated Trogoptosis and enhances antigen cross-presentation”. *Oncoimmunology* 2020;9:1824323.
- van Bommel PE, He Y, Schepel I, *et al*. “Cd20-selective inhibition of Cd47-SIRPα “don’t eat me” signaling with a Bispecific antibody-derivative enhances the anticancer activity of Daratumumab, Alemtuzumab and Obinutuzumab”. *Oncoimmunology* 2018;7:e1386361.
- Gao Z, Wang H, Lin F, *et al*. Cd73 promotes proliferation and migration of human Cervical cancer cells independent of its enzyme activity. *BMC Cancer* 2017;17.
- Biscardi JS, Maa MC, Tice DA, *et al*. C-SRC-mediated Phosphorylation of the Epidermal growth factor receptor on Tyr845 and Tyr1101 is associated with modulation of receptor function. *J Biol Chem* 1999;274:8335–43.
- Dianzani U, Redoglia V, Bragardo M, *et al*. Co-stimulatory signal delivered by Cd73 molecule to human Cd45Rahicd45Rolo (naive) Cd8+ T lymphocytes. *J Immunol* 1993;151:3961–70.
- Airas L, Niemelä J, Salmi M, *et al*. Differential regulation and function of Cd73, a Glycosyl-Phosphatidylinositol-linked 70-kD adhesion molecule, on lymphocytes and endothelial cells. *J Cell Biol* 1997;136:421–31.
- Samanta D, Park Y, Ni X, *et al*. Chemotherapy induces enrichment of Cd47+/Cd73+/Pd11+ immune evasive triple-negative breast cancer cells. *Proc Natl Acad Sci U S A* 2018;115:E1239–48.
- Ujházy P, Klobusická M, Babusiková O, *et al*. Ecto-5'-Nucleotidase (Cd73) in multidrug-resistant cell lines generated by doxorubicin. *Int J Cancer* 1994;59:83–93.
- Loi S, Pommey S, Haibe-Kains B, *et al*. Cd73 promotes anthracycline resistance and poor prognosis in triple negative breast cancer. *Proc Natl Acad Sci U S A* 2013;110:11091–6.
- Dietrich F, Figueiró F, Filippi-Chiela EC, *et al*. Ecto-5'-Nucleotidase/ Cd73 contributes to the Radiosensitivity of T24 human bladder cancer cell line. *J Cancer Res Clin Oncol* 2018;144:469–82.

Bispecific antibody CD73xEGFR inhibits the CD73/adenosine immune checkpoint in a tumor-directed manner and concurrently counteracts pro-oncogenic activities of CD73 and EGFR



Authors

Emily M. Ploeg, Douwe F. Samplonius, Xiao Xiong, Xiurong Ke, Mark A.J.M. Hendriks, Isabel Britsch, Anne P. van Wijngaarden, Hao Zhang, Wijnand Helfrich.

Correspondence

w.helfrich@umcg.nl

In Brief

In vitro treatment of CD73^{pos}/EGFR^{pos} cancer cells with bsAb CD73xEGFR induced rapid internalization of antigen/antibody complexes, which resulted in a prolonged concurrent displacement of both CD73 and EGFR from the cancer cell surface. This treatment potentially inhibited the proliferative and migratory capacity of cancer cells *in vivo* and sensitized them to the cytotoxicity activity of various chemotherapeutic agents and that of ionizing radiation *in vitro*. Moreover, in a tumor model using immunocompetent mice inoculated with syngeneic EGFR^{pos}/CD73^{pos} tumor cells, treatment with bsAb CD73xEGFR outperformed oleclumab in restoring the anticancer activity of ADO-suppressed T cells.

SUPPLEMENTARY DOCUMENTATION

Bispecific antibody CD73xEGFR inhibits the CD73/adenosine immune checkpoint in a tumor-directed manner and concurrently counteracts pro-oncogenic activities of CD73 and EGFR

Emily M. Ploeg¹, Douwe F. Samplonius¹, Xiao Xiong^{2,3}, Xiurong Ke^{1,4}, Mark A.J.M. Hendriks¹, Isabel Britsch¹, Anne P. van Wijngaarden¹, Hao Zhang^{5,6}, Wijnand Helfrich¹.

- 1 Department of Surgery, Laboratory for Translational Surgical Oncology, University of Groningen, University Medical Center Groningen, Groningen, The Netherlands.
- 2 Department of Urology, Guangdong Second Provincial General Hospital, Guangzhou, Guangdong, China.
- 3 Faculty of Medical Science and Integrated Chinese and Western Medicine Postdoctoral research station, Jinan University, Guangzhou, Guangdong, China
- 4 Shantou University Medical College, Shantou, Guangdong, China.
- 5 Department of General Surgery, The First Affiliated Hospital of Jinan University, and Institute of Precision Cancer Medicine and Pathology, School of Medicine, Jinan University, Guangzhou, Guangdong, China.
- 6 Minister of Education Key Laboratory of Tumor Molecular Biology, Jinan University, Guangzhou, Guangdong, China.

GRAPHICAL ABSTRACT

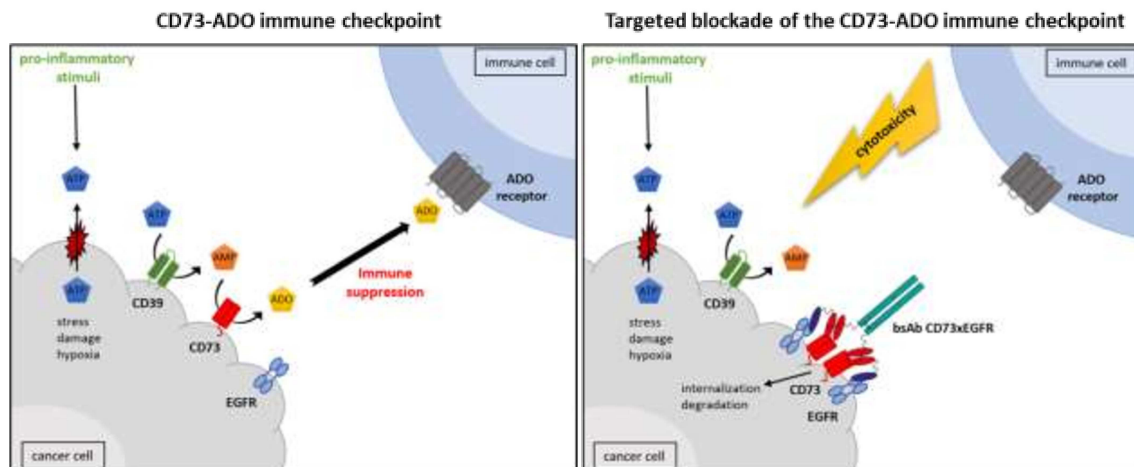


Table of contents

Additional material and methods.....	3
Supplementary figure 1: bsAb CD73xEGFR simultaneously binds to CD73 and EGFR.....	5
Supplementary figure 2: Relative CD73 and EGFR expression levels on 16 cell lines.....	5
Supplementary figure 3: bsAb CD73xEGFR simultaneously binds to CD73 and EGFR.....	6
Supplementary figure 4: bsAb CD73xEGFR induces co-internalization of both CD73 and EGFR from the cancer cell surface.....	6
Supplementary figure 5: Oleclumab treatment increases EGFR and HER2 expression levels in cancer cells.....	7
Supplementary figure 6: bsAb CD73xEGFR co-internalize CD73 and EGFR in an EGFR-directed manner.....	8
Supplementary figure 7: bsAb CD73xEGFR potently inhibits the enzyme activity of CD73.....	8
Supplementary figure 8: bsAb CD73xEGFR restores anticancer activities of ADO-suppressed T-cells...	9
Supplementary figure 9: <i>In vitro</i> assessment bsAb CD73xEGFR using CT26 murine cancer cells.....	9
Supplementary figure 10: bsAb CD73xEGFR reduces syngeneic tumor size in immunocompetent mice.....	10
Supplementary figure 11: bsAb CD73xEGFR increases the tumor-infiltrating capacity of lymphocytes in immunocompetent tumor-bearing mice.....	11
Supplementary figure 12: bsAb CD73xEGFR increases the tumor-infiltrating capacity of leukocytes in immunocompetent tumor-bearing mice.....	12
Supplementary figure 13: bsAb CD73xEGFR-treatment induces no or minimal systemic toxicity in immunocompetent mice.....	13
Supplementary figure 14: bsAb CD73xEGFR inhibits the proliferative capacity of cancer cells.....	14
Supplementary figure 15: bsAb CD73xEGFR reduces cell colony formation of carcinoma cells.....	14
Supplementary figure 16: Treatment with bsAb CD73xEGFR inhibits the proliferative capacity of xenografted cancer cells in immunodeficient mice.....	15
Supplementary figure 17: bsAb CD73xEGFR sensitizes cancer cells towards treatment with chemotherapeutic agents.....	16

Additional material and methods

Construction of bsAb CD73xEGFR-IgG2silent

DNA fragments encoding scFvCD73 and VHH EGFR were generated by commercial gene synthesis service (Genscript) based on published VH and VL sequence data from oleclumab (4) and EGFR-directed camelid single-domain antibody fragment NRC-sdAb028 (8), respectively. For construction of bsAb CD73xEGFR-IgG2silent and controls eukaryotic expression plasmid pbsAb was used, which contains 3 consecutive multiple cloning sites (MCS). MCS#1 and MCS#2 are interspersed by a 22 amino acid flexible linker and used for directional and in-frame insertion of DNA fragments encoding scFvCD73, VHH EGFR. MCS#3 contain DNA fragments encoding human Fc IgG2-silent, which mitigates immune effector functions. Analogously, pbsAb-CD73xMock-IgG2s encoding bsAb CD73xMock-IgG2s was constructed by replacing VHH EGFR in pbsAb-CD73xEGFR-IgG2s by scFvMCSP directed against CSPG4. Likewise, pbsAb-MockxEGFR-IgG2s encoding bsAb MockxEGFR-IgG2s was constructed by replacing scFvCD73 in pbsAb-CD73xEGFR-IgG2s by scFv4-4-20 directed against fluorescein. Plasmid pbsAb-MockxMock-IgG2s encoding bsAb MockxMock-IgG2s was constructed by replacing scFvCD73 in pbsAb-CD73xMock-IgG2s by scFv4-4-20.

Immunoblot analysis

Protein content of lysed cell samples was determined using the Bradford method after which samples with equal protein content (20 µg) were subjected to SDS/PAGE. In short, samples were mixed with 4x Laemmli sample buffer (containing 355 mM 2-mercaptoethanol) and heated at 95°C for 5 min. Subsequently, the separated proteins were transferred to a 0.45 µm nitrocellulose membrane. Separate lanes of the membrane were incubated with indicated primary antibodies at 4°C for 16 h and subsequently incubated with an appropriate horseradish peroxidase-conjugated secondary antibody at room temperature for 2 h. Immunoreactive bands were visualized with SuperSignal West Pico Chemiluminescent Substrate (ThermoFisher) and analyzed using Bio-Rad ImageLab.

Assessment dual binding activity of bsAb CD73xEGFR

The capacity of bsAb CD73xEGFR to simultaneously bind to CD73 on one cell type and EGFR on a proximal other cell type was assessed by flow cytometry. In short, CD73^{pos}/EGFR^{pos} FaDu cancer cells (DiO-labeled) were co-cultured with CD73^{pos}/EGFR^{neg} CHO.CD73 (DiD-labeled) or CD73^{neg}/EGFR^{neg} CHO.Mock (DiD-labeled) and incubated with bsAb CD73xEGFR (1 µg/ml) at 4°C for 45 min. The percentage of DiO^{pos}/DiD^{pos} cell clusters was evaluated by flow cytometry.

Assessment capacity of bsAb CD73xEGFR to inhibit the CD73 enzyme activity

CD73 enzyme activity was assessed using a colorimetric malachite green-based phosphate assay kit (ab65622, Abcam). Quantification of free orthophosphate (Pi) by this assay is based on the green complex that is formed when Pi interacts with Malachite Green and molybdate. In short, cancer cells were treated with increasing concentrations (0.01 - 10 µg/ml) bsAb CD73xEGFR or controls at 37°C for 24 h. Subsequently, cancer cells were washed (20 mM HEPES, 120 mM NaCl, 5 mM KCl, 2 mM MgCl₂, 10 mM Glucose, pH 7.4) to remove the phosphate buffer-containing cell culture medium. Next, cancer cells were resuspended in the same HEPES wash buffer supplemented with 100 µM AMP (Sigma-Aldrich) and incubated at 37°C for a period of 40 min. Next, the supernatant was harvested and mixed with the malachite green reagent after which color development was evaluated by measuring the absorbance at 650 nm using a microplate reader (VERSA max, Molecular Devices). Final Pi concentration was corrected by subtraction of background levels.

The % of enzyme inhibition was calculated by the following formula:

$$\% \text{ of CD73 enzyme inhibition} = 100 - \left(\frac{X}{\text{OD650}_{\text{max}}} \right) * 100$$

X = is the OD value measured in a given experiment minus the background (OD650_{exp} - OD650_{background})
 OD650_{max} = the amount of Pi present in the conditioned supernatant in the absence of bsAb

Multiplexed immunofluorescence to assess tumor-infiltrating leukocytes

Multiplexed immunofluorescence to evaluate T cell and macrophage populations in tumors resected from immunocompetent mice was performed as described previously (10).

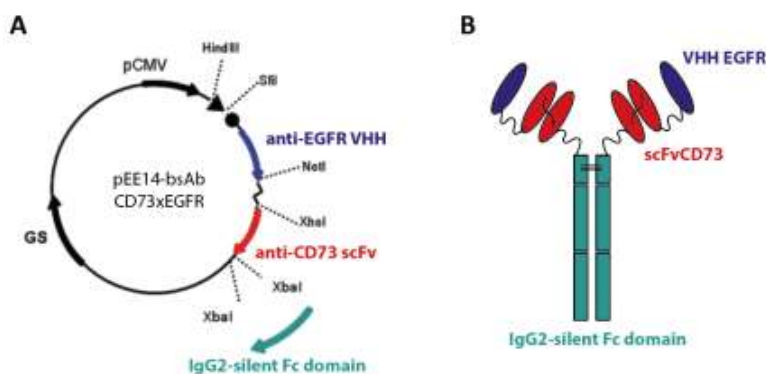
All excised tumors were identically processed for multiplexed immunofluorescence or histological analysis. For histological analysis, 3 tumors per treatment group and 3 images per tumor were analyzed to quantify the amount of tumor-infiltrating immune cells. To control the comparability of the slice section between animals, excised tumors were dissected into two equally sized halves one of which was formalin-fixed and paraffine-embedded (FFPE) according to standard procedures. FFPE tumor specimens were mounted cut-surface downward on glass slides. Subsequently, successive sections were cut and compared from each tumor sample by multiplexed immunofluorescence or histology.

Histological assessment of signs of toxicity

Various organs and tissues were fixed in 10% formalin, embedded in paraffin, and stained with hematoxylin and eosin (H&E). Histological images were evaluated for signs of toxicity by two independent pathologists.

EGFR phosphorylation antibody array

Cancer cells were incubated with bsAb CD73xEGFR, bsAb MockxEGFR or oleclumab (all 1 µg/ml) for 24 h and washed twice with cold PBS. Protein content of lysed cell samples was determined using the Bradford method. The Human EGFR Phosphorylation Antibody Array (Abcam, ab134005) was used according to protocol for detection of 17 phosphorylated human EGF receptors; EGFR (Tyr845), EGFR (Tyr992), EGFR (Tyr1045), EGFR (Tyr1068), EGFR (Tyr1086), EGFR (Tyr1148), EGFR (Tyr1173), EGFR (Ser1046/1047), EGFR (Ser1070), ErbB2 (Tyr877), ErbB2 (Tyr1112), ErbB2 (Tyr 1221/1222), ErbB2 (Tyr1248), ErbB2 (Thr686), ErbB2 (Ser1113), ErbB3 (Tyr1289), and ErbB4 (Tyr1284). Pictures were taken with Bio-Rad Chemidoc and analyzed using Bio-Rad ImageLab.



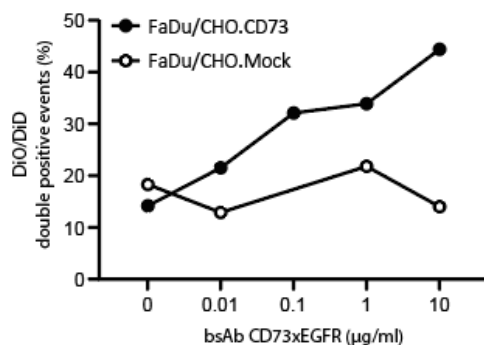
Supplementary figure 1: bsAb CD73xEGFR simultaneously binds to CD73 and EGFR

(A) Topology of expression plasmid pbsAb encoding bsAb CD73xEGFR-IgG2s and (B) schematic depiction of bsAb CD73xEGFR-IgG2s protein.

Cancer type	CD73	EGFR
Breast cancer		
MDA-MD-231	++++	++
SK-BR-3	++	++
Lung cancer		
H292	++++	+++
H322	++	++
A549	++	++
H1650	++	++
Colon cancer		
DLD1	+++	++
Widr	+	+
Head and neck cancer		
FaDu	+	++++
Ovarian cancer		
OvCAR3	+++	+++
PEA1	+++	+++
Prostate cancer		
PC3M	+	+
Epidermoid cancer		
A431	++	++++
Melanoma		
A2058	++	-
SK-MEL-28	++++	-
A375m	+/-	-

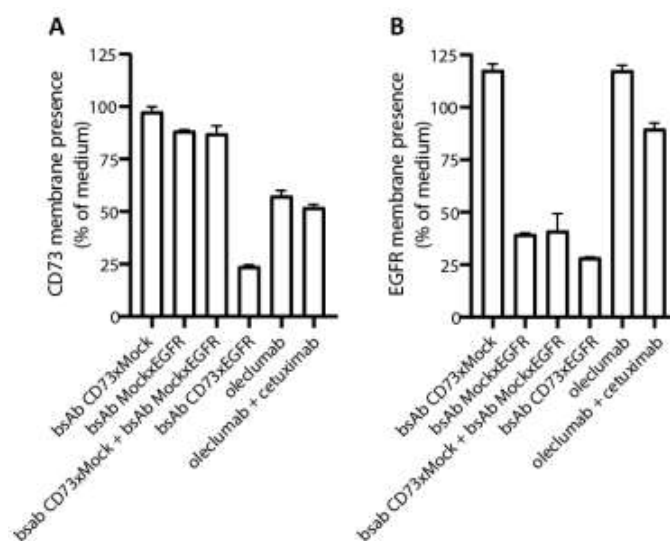
Supplementary figure 2: Relative CD73 and EGFR expression levels on 16 cell lines

Relative CD73 and EGFR expression levels on a panel of 16 cell lines used in this study. - = MFI < 5, + = MFI 5 – 20, ++ = MFI 20 – 200, +++ = MFI 200 – 500, ++++ = MFI > 500. Expression levels were analyzed by flow cytometry.



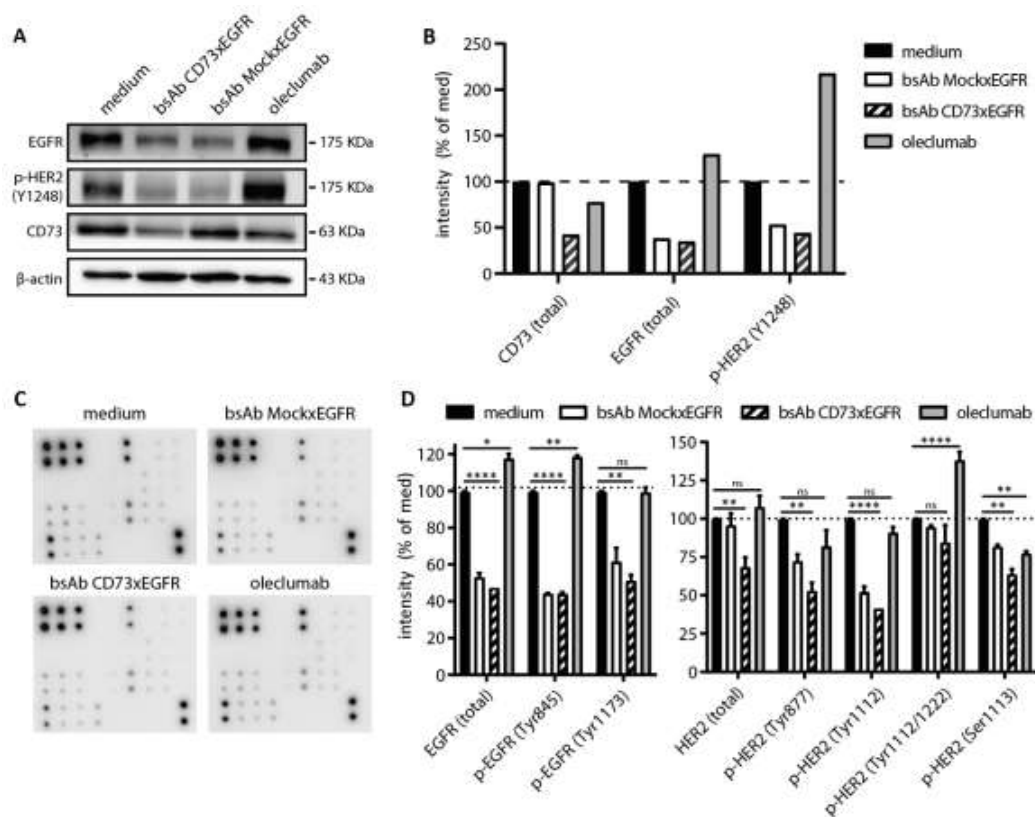
Supplementary figure 3: bsAb CD73xEGFR simultaneously binds to CD73 and EGFR

Binding of bsAb CD73xEGFR (0.01 – 10 µg/ml) cellularly bridged FaDu cancer cells (DiO-labeled) and CHO.CD73 (black) or CHO.Mock cells (white) (DiD-labeled). Binding was analyzed by flow cytometry. Data shown in the graph represent mean ± SD, n = 3 (2 technical replicates).



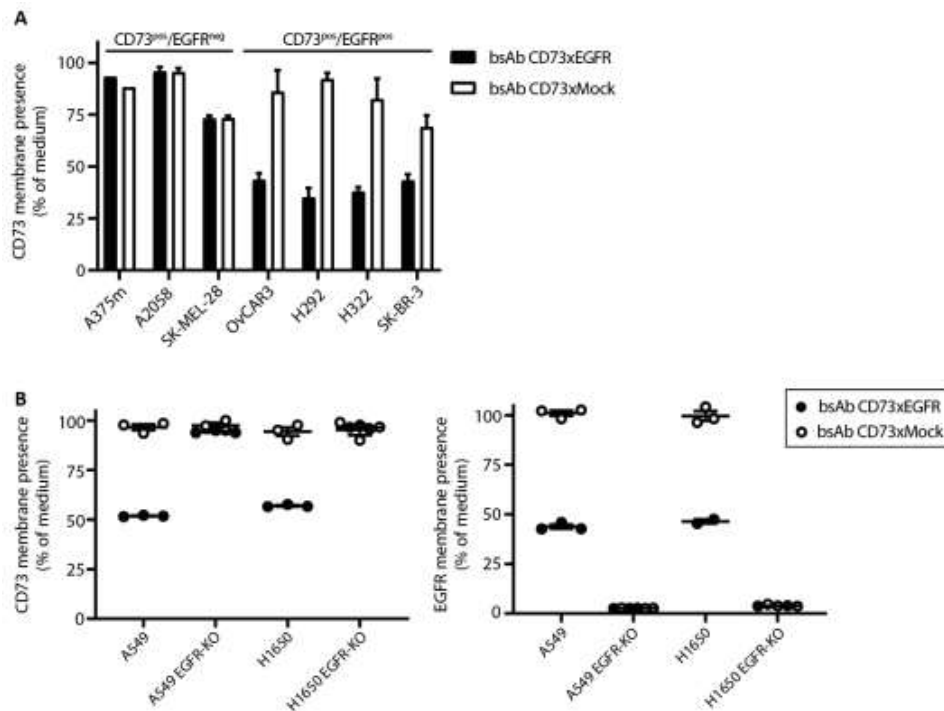
Supplementary figure 4: bsAb CD73xEGFR induces co-internalization of both CD73 and EGFR from the cancer cell surface

Residual (A) CD73 and (B) EGFR membrane presence on H292 cells after treatment with bsAb CD73xEGFR or controls (1 µg/ml) for 24 h. Data shown in the graph represent mean ± SD, n = 3 (2 technical replicates).



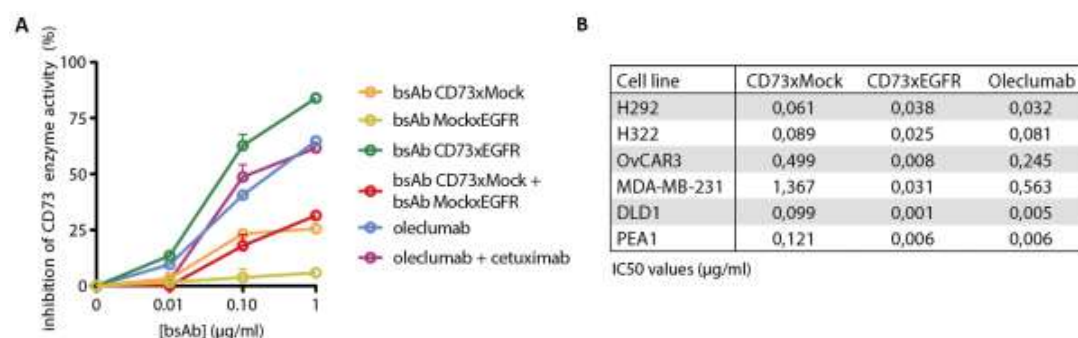
Supplementary figure 5: Oleclumab treatment increases EGFR and HER2 expression levels in cancer cells

Representative images of (A) immunoblot analysis and subsequent (B) quantification of CD73, EGFR, phosphorylated-HER2 (Y1248) and β -actin expression by H292 cancer cells after treatment with bsAb CD73xEGFR or controls (1 μ g/ml) at 37°C for 24 h. Equal protein concentration (20 μ g) of each sample was loaded. Representative pictures of (C) EGFR growth factor array and subsequent (D) quantification of (phosphorylated) EGFR and (phosphorylated) HER2 expressed by H292 cancer cells after treatment with bsAb CD73xEGFR or controls (1 μ g/ml) at 37°C for 24 h. Pictures were analyzed using Bio-Rad ImageLab software. Statistical analysis in D was performed using one-way ANOVA followed by Tukey post-hoc test (* $p < .05$, ** $p < .01$, **** $p < .0001$).



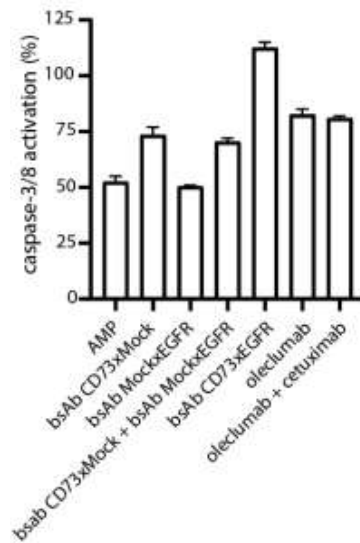
Supplementary figure 6: bsAb CD73xEGFR co-internalize CD73 and EGFR in an EGFR-directed manner

(A) Residual CD73 cell surface expression levels of CD73^{pos}/EGFR^{neg} (A375m, A2058, and SK-MEL-28) and CD73^{pos}/EGFR^{pos} (OvCAR3, H292, H322, and SK-BR-3) cell lines after treatment with bsAb CD73xEGFR or bsAb CD73xMock (both 1 μ g/ml) for 24 h. (B) Residual CD73 and EGFR cell surface expression levels of parental cancer cells (A549 and H1650) and corresponding EGFR-KO variants thereof after treatment with bsAb CD73xEGFR or bsAb CD73xMock (both 1 μ g/ml) for 24 h. All experiments were analyzed by flow cytometry. All graphs: n = 3 (3 technical replicates). All graphs represent mean \pm SD.



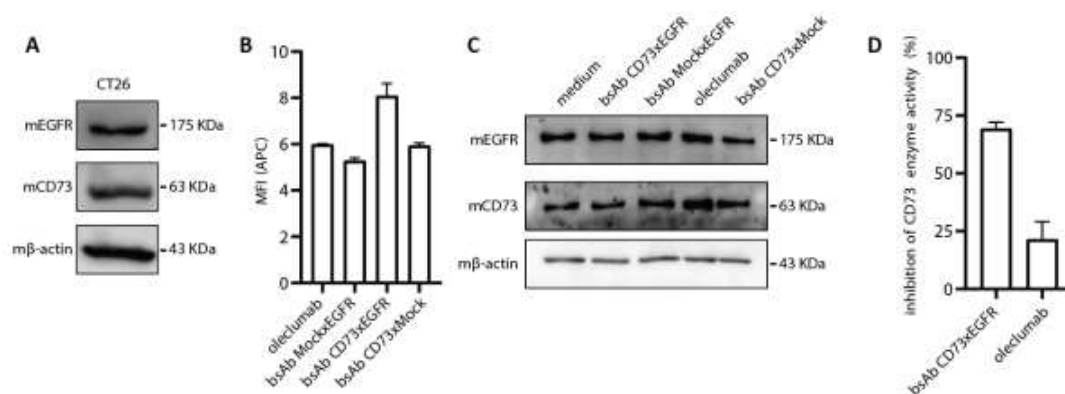
Supplementary figure 7: bsAb CD73xEGFR potently inhibits the enzyme activity of CD73

(A) Percentage of inhibition CD73 enzyme activity on H292 cells after treatment with bsAb CD73xEGFR or controls (0.01 – 10 μ g/ml) for 24 h. (B) IC₅₀ values (μ g/ml) calculated for a panel of 6 carcinoma cell lines that were treated with bsAb CD73xEGFR or controls (0.01 - 10 μ g/ml) for 24 h and then evaluated for their capacity to inhibit CD73 enzyme activity. Graph A represents mean \pm SD, n = 2 (3 technical replicates).



Supplementary figure 8: bsAb CD73xEGFR restores anticancer activities of ADO-suppressed T-cells

Caspase-3/8 activation (apoptotic cancer cell death) in PC3M cancer cells subjected to bsAb CD3xEpCAM-redirceted PBMCs at an effector (E) to target (T) cell ratio of 4:1. PBMCs were incubated with (or without) AMP, in the presence or absence of bsAb CD73xEGFR, olectumab, or controls (all 1 μ g/ml). Caspase-3/8 activation was evaluated using live-cell imagine technology. Graph represents mean \pm SD, n = 3 (4 technical replicates).



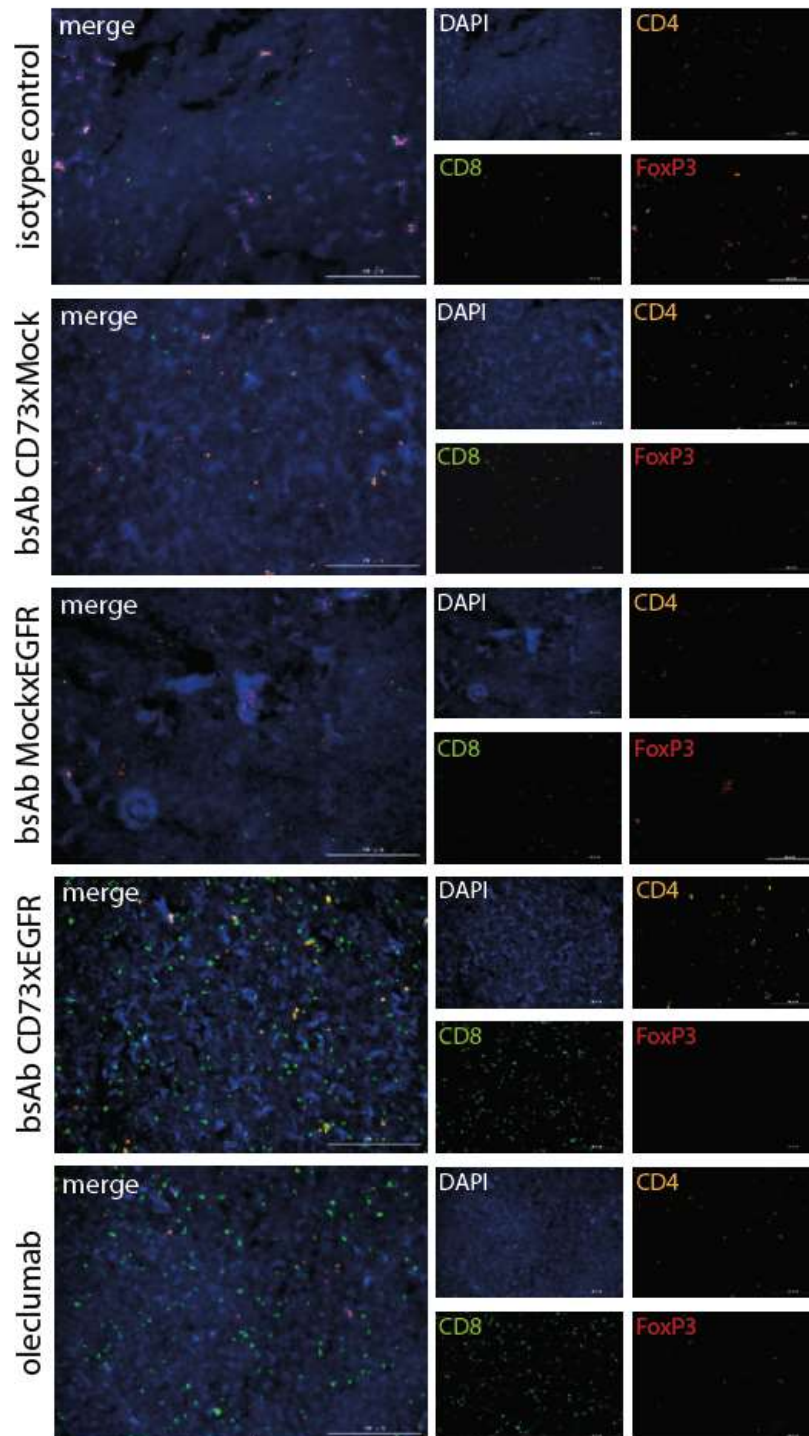
Supplementary figure 9: *In vitro* assessment bsAb CD73xEGFR using CT26 murine cancer cells

(A) Immunoblot analysis of murine CD73 (mCD73), murine EGFR (mEGFR), and murine β -actin (m β -actin) expression levels in CT26 murine cancer cells (cell lysate protein 40 μ g/lane). (B) Flow cytometric analysis of binding of bsAb CD73xEGFR or controls (1 μ g/ml) to CT26 cancer cells. Indicated MFI levels are corrected for isotype control background levels. (C) Immunoblot analysis of mCD73, mEGFR, and m β -actin expression by CT26 cells after treatment with bsAb CD73xEGFR or controls (1 μ g/ml) at 37°C for 24 h. Equal amounts of protein (40 μ g) of each sample were loaded per lane. (D) Percentage inhibition of mCD73 enzyme activity on CT26 cells after treatment with bsAb CD73xEGFR or controls (1 μ g/ml) at 37°C for 24 h. Graph B: n = 1 (3 technical replicates), graph D: n = 3 (2 technical replicates). All graph represent mean \pm SD.



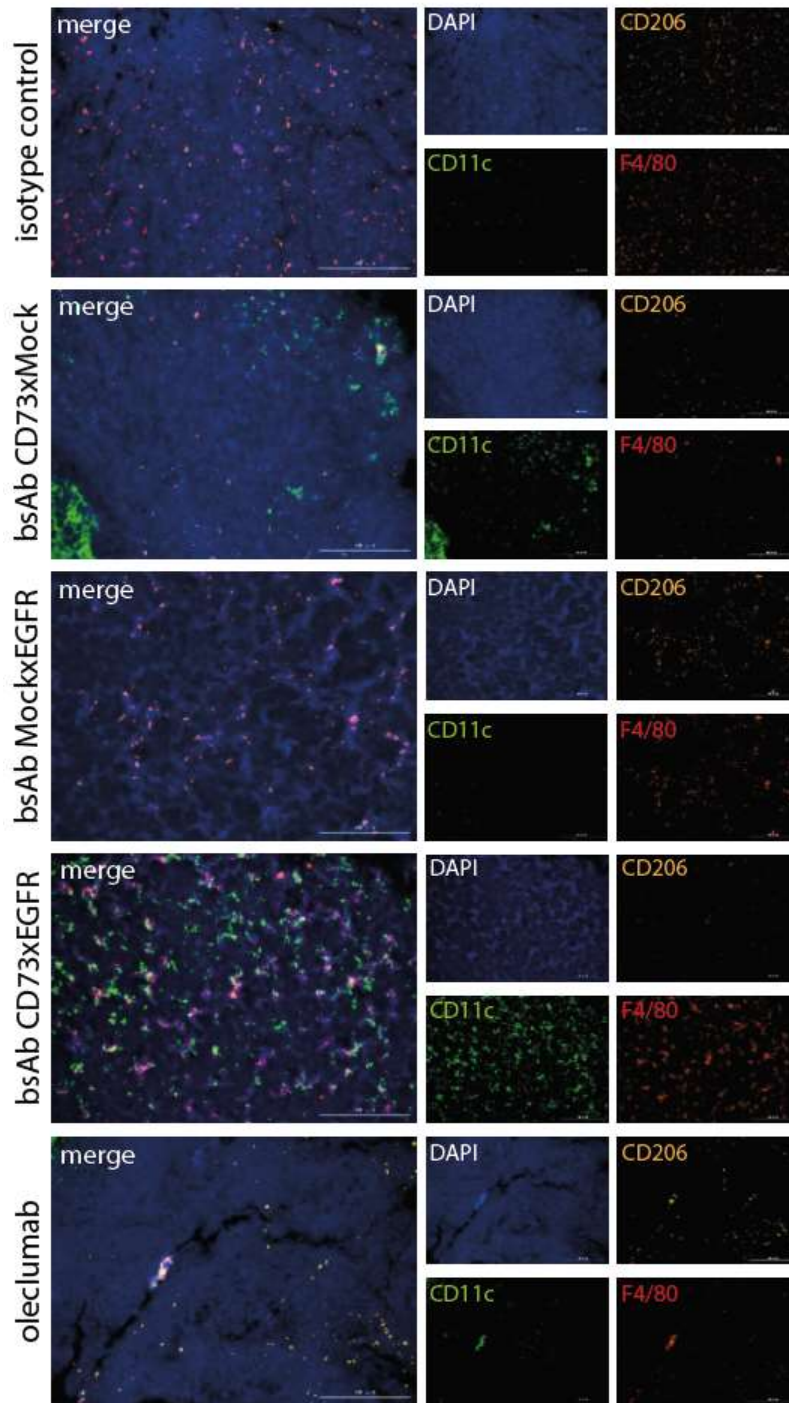
Supplementary figure 10: bsAb CD73xEGFR reduces syngeneic tumor size in immunocompetent mice

Representative picture of CT26 syngeneic tumors, harvested from BALB/c mice 21 d post tumor injection. Mice were treated I.P. with bsAb CD73xEGFR or controls (7.5 mg/kg) on day 4, 7, 10 and 14. 5 tumors per treatment-group are shown. Scale bar = 1 cm.



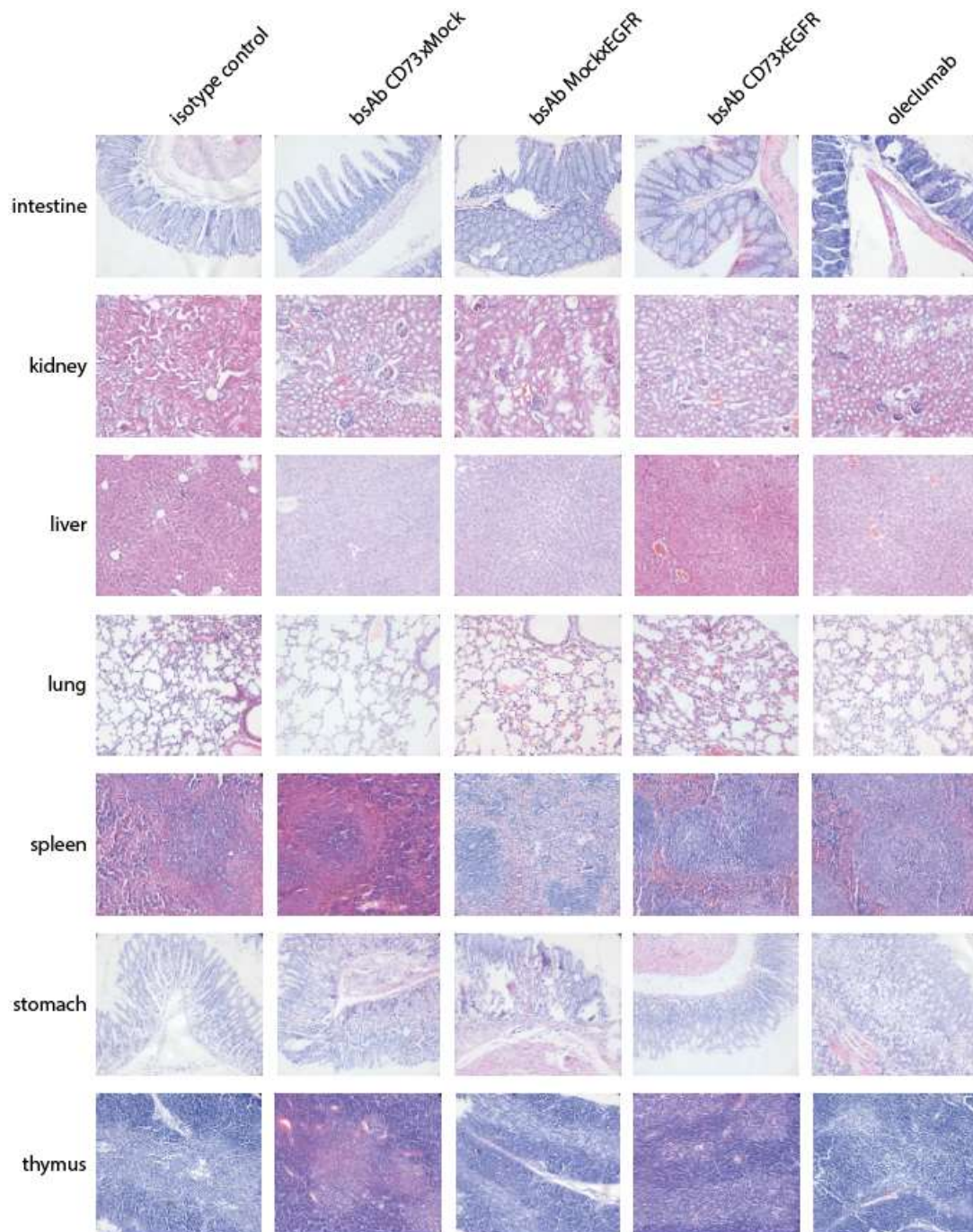
Supplementary figure 11: bsAb CD73xEGFR increases the tumor-infiltrating capacity of lymphocytes in immunocompetent tumor-bearing mice

Representative images of multiplexed immunofluorescence staining for CD4, CD8, and FoxP3 in CT26-tumor sections, harvested 21 d post tumor inoculation. Mice were treated I.P. with bsAb CD73xEGFR or controls (7.5 mg/kg) on day 4, 7, 10 and 14. Scale bar = 200 μ m.



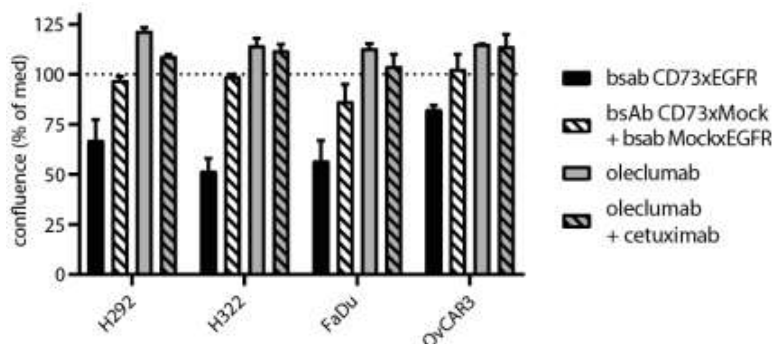
Supplementary figure 12: bsAb CD73xEGFR increases the tumor-infiltrating capacity of leukocytes in immunocompetent tumor-bearing mice

Representative images of multiplexed immunofluorescence staining for CD206, CD11c, and F4/80 in CT26-tumor sections, harvested 21 d post tumor inoculation. Mice were treated I.P. with bsAb CD73xEGFR or controls (7.5 mg/kg) on day 4, 7, 10 and 14. Scale bar = 200 μ m.



Supplementary figure 13: bsAb CD73xEGFR-treatment induces no or minimal systemic toxicity in immunocompetent mice

Representative histological images (H&E staining) of various organs and tissues harvested 21 d post tumor inoculation from mice treated with bsAb CD73xEGFR, oleclumab, or controls. Mice were treated I.P. with bsAb CD73xEGFR or controls (7.5 mg/kg) on day 4, 7, 10 and 14. Pictures were taken at 200 x magnification.

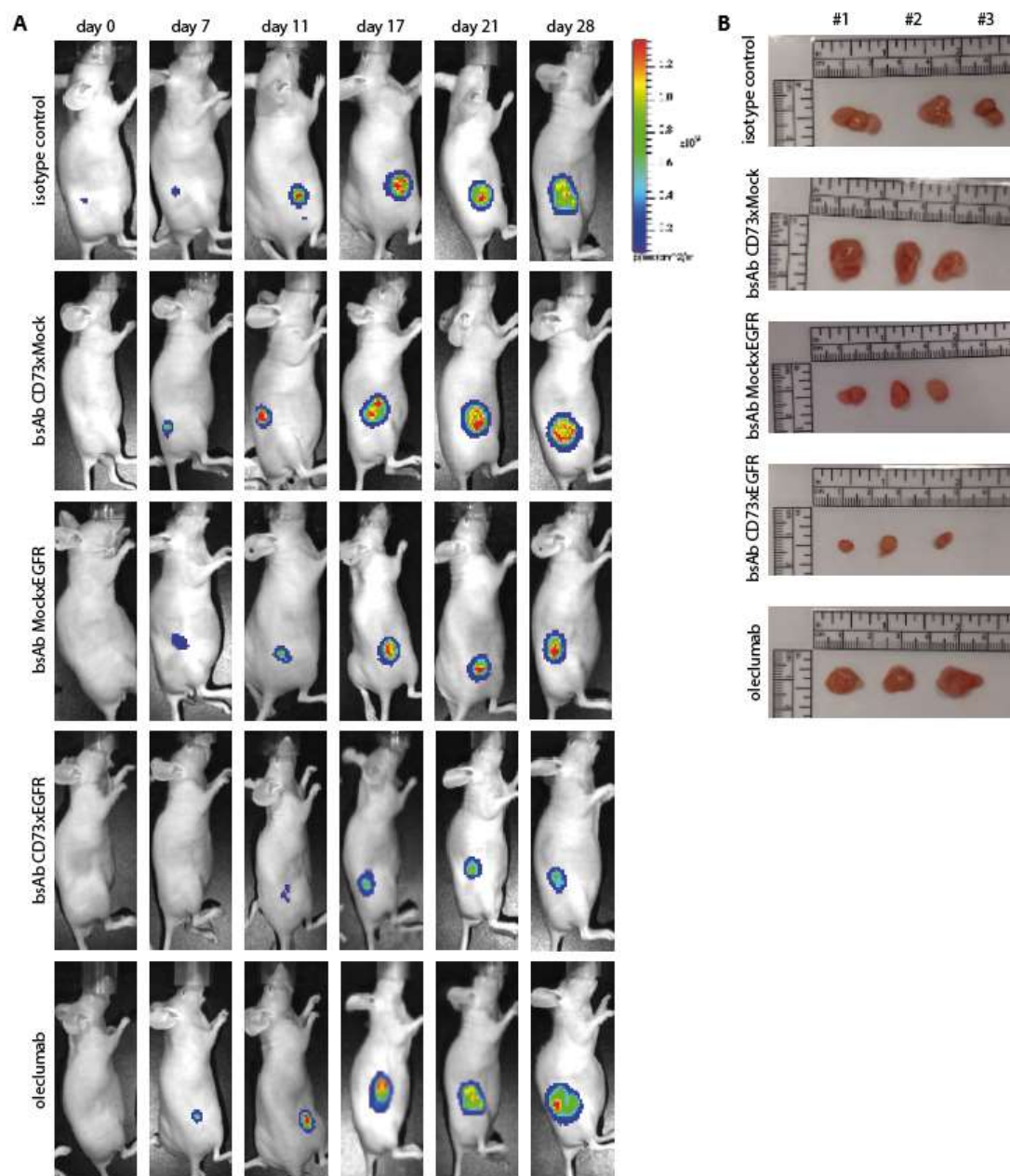


Supplementary figure 14: bsAb CD73xEGFR inhibits the proliferative capacity of cancer cells
Proliferation assay in which a panel of cell lines (H292, H322, FaDu, and OvCAR3) was incubated with bsAb CD73xEGFR or controls (1 $\mu\text{g}/\text{ml}$). The percentage of cell confluence was evaluated after culturing for 72 h. Graph represent mean \pm SD, n = 3 (2 technical replicates).

Cell line	antibody			
	CD73xMock	MockxEGFR	CD73xEGFR	oleclumab
OvCAR3	9,193 \pm	1,254 \pm	0,653 \pm	24,33 \pm
IC50/SDe	1,821	0,258	0,163	7,667
H322	4,760 \pm	1,257 \pm	0,775 \pm	9,381 \pm
IC50/SDe	0,834	0,250	0,106	2,311
H292	1,228 \pm	0,409 \pm	0,165 \pm	15,07 \pm
IC50/SDe	0,202	0,065	0,032	3,118

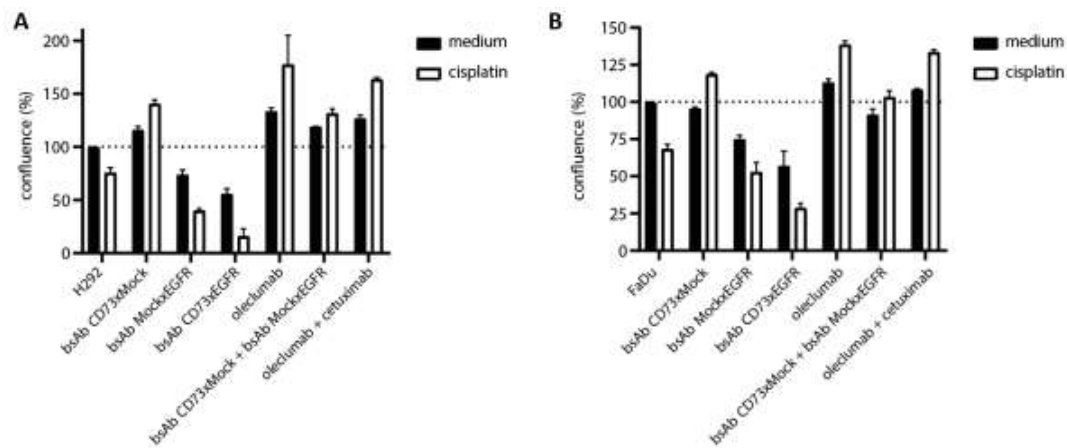
IC50 and SDe values ($\mu\text{g}/\text{ml}$) clonogenic assay

Supplementary figure 15: bsAb CD73xEGFR reduces cell colony formation of carcinoma cells
IC₅₀ values ($\mu\text{g}/\text{ml}$) calculated for a OvCAR3, H322 and H292 cell lines that were treated with bsAb CD73xEGFR or controls (0.01 - 10 $\mu\text{g}/\text{ml}$) at 37 $^{\circ}\text{C}$ for 14 d and subsequently assessed for the number of cell colonies.



Supplementary figure 16: Treatment with bsAb CD73xEGFR inhibits the proliferative capacity of xenografted cancer cells in immunodeficient mice

(A) Representative bioluminescent images of athymic nude mice (CrI:NU(NCr)-Foxn^{nu}) inoculated S.C. in the flank with human H292-luc2 non-small lung cancer cells on day 0, 7, 11, 17 and 28 post tumor inoculation. Mice were treated I.P. with bsAb CD73xEGFR or controls (7.5 mg/kg) on day 7, 10 and 17. (B) Representative pictures of 3 excised H292-luc2 tumors after indicated treatment, 28 d post tumor inoculation. Scale bar = 1 cm.



Supplementary figure 17: bsAb CD73xEGFR sensitizes cancer cells towards treatment with chemotherapeutic agents

Cell confluence of H292 (A) or FaDu (B) cancer cells treated (or not) with bsAb CD73xEGFR (1 $\mu\text{g}/\text{ml}$) or controls in the presence (or absence) of cisplatin (1 $\mu\text{g}/\text{ml}$) at 37 $^{\circ}\text{C}$ for 4 d and then evaluated using live cell imaging by taking pictures at 4x magnification every 6 h. All graphs represent mean \pm SD. Graph A - B: n = 3 (2 technical replicates). All graph represent mean \pm SD.